CIRCUITRY AND TECHNOLOGY MATCHING TO THE PATH FUNCTIONALITY IN THE OPTICAL NODE

Project title	**Photonics technologies for ProgrAmmable transmission and switching modular systems based on Scalable Spectrum/space aggregation for future aglle high capacity metrO Networks**
Project acronym	**PASSION**
Grant number	**780326**
Funding scheme	**Research and Innovation Action - RIA**
Project call	**H2020-ICT-30-2017 Photonics KET 2017 Scope i. Application driven core photonic technology developments**
Work Package	**WP4**
Lead Partner	**TU/e**
Contributing Partner(s)	**EFP, ETRI, TID, POLIMI, OPSYS**
Nature	**R**
Dissemination level	**PU (Public)**
Contractual delivery date	**31/03/2018**
Actual delivery date	**30/03/2018**
Version	**1.0**

History of changes

Version	Date	Comments	Main Authors
0.1	24/03/2018		N. Tessema, N. Calabretta, P. Stabile (TUE), S. Ben-Ezra (OPSYS), K. Solis-Trapala, E. Kleijn (EFP),

			H. Jung (ETRI)
0.2	28/3/2018	Technical review	S. Ben-Ezra (OPSYS)
0.3	28/3/2018	Quality review	M. Svaluto Moreolo (CTTC)
1.0	30/3/2018	Final version	N. Tessema (TUE), P. Boffi (POLIMI)

Disclaimer

This document contains confidential information in the form of the PASSION project findings, work and products and its use is strictly regulated by the PASSION Consortium Agreement and by Contract no. 780326.

Neither the PASSION Consortium nor any of its officers, employees or agents shall be responsible or liable in negligence or otherwise howsoever in respect of any inaccuracy or omission herein.

The contents of this document are the sole responsibility of the PASSION consortium and can in no way be taken to reflect the views of the European Union.

This project has received funding from the European Union's Horizon 2020 Research and Innovation Programme under Grant Agreement No 780326.

TABLE OF CONTENTS

TABLE OF FIGURES

EXECUTIVE SUMMARY

PASSION introduces new photonic technologies and devices for supporting agile metro networks, capable of enabling target capacities of Tb/s per channel, 100 Tb/s per link and Pb/s per node over increased transport distances in the range of few hundreds of kilometers. The modularity and programmability (via Software Defined Networks: SDN) of the system and subsystem components of the node is used to achieve the flexibility and agility level demanded by the dynamic traffic, channel bandwidth/path/state/energy requirements of the metro network. Development of energy-efficient and small-footprint switching technologies for a node featuring functional aggregation/disaggregation, together with switching in the space and wavelength domain will be used to handle up to 1 Pb/s capacity. PASSION's goal is achieved by exploiting VCSEL sources, each one operating at a different WDM wavelength in the C-band, directly modulated to obtain up to 50 Gb/s rate to target up to 8 Tb/s capacity per polarization. 16 Tb/s per spatial channel are achieved exploiting polarization-division multiplexing, while the spatial dimension of 7 multi core fibers (MCF) or 7 fibers in a bundle allows enabling up to 112 Tb/s aggregated capacity per link.

The applicability of the PASSION switching node for real life scenario is presented via description of two use cases considering the traffic properties in a stadium where a large collection of people demand high bandwidth connectivity during the game. The capability to switch wavelengths when needed is explained. The PASSION node matched for Metro Access and Metro Regional applications is used also to give 5G back-haul support together passive optical network (PON).

Section 2 illustrates the switching node functionalities used in *Photonic switches*, *Add switches*, *Aggregate/disaggregate switches*, and *Multicast switches (MCS).* The use of multicast switches (MCS) along with coherent reception provides color-less, direction-less and contention-less performance. The photonic switches provide "high-level switching" at any input port (corresponds to add traffic/ express-in traffic) to any output port (corresponds to drop or express-out traffic). A high level of flexibility is needed to be able to fully configure the data traffic while being able to add/drop on the fly and guarantee full link usage at the same time. The Aggregation/disaggregation switch functionality supports this flexibility for maximizing resource utilization by aggregating/disaggregating traffic back to the express path or to the drop path. The drop traffic is directly connected to an array of multi-cast switches and enable efficient utilization of the coherent receiver modules.

In Section 3, the circuit implementation of the proposed switching architecture is given. The photonic switch is implemented as a photonic switch matrix with a target platform on polymer planar light wave circuit (PLC) for low cost and compact footprint implementation. The PASSION cross-bar photonic switch will be comprised of a polymer thermo-optic 1x2 the total internal reflection (TIR) switch as a unit switching element, which has an asymmetric Y-branch of multimode polymer waveguides and a heater electrode to induce the TIR by thermo-optic effect on the branched node. The core of Aggregate/disaggregate switches and Add switches is based on Indium phosphide (InP) WSS (wavelength selective switches) which are implemented by using a wavelength blocking unit. The wavelength blocking unit consists of AWG demultiplexer, SOA gate switches and AWG multiplexer. In addition, SOA booster amplifiers in conjunction with power splitters (PS) are employed in WSS implementation. The advantage of implementing those function with SOAs are the fast switch and the on-chip amplification to realize lossless switching sub-systems. The MCS implementation is based on broadcast and select principle with booster SOA, PS and wavelength switches. InP Coherent receiver technology will be leveraged to realize multi-channel, polarization diverse and polarization independent receiver array.

In Section 4, the switching architecture based on modularity approach for scalable performance employed in the optical node implementation is presented. In this way, each switching module has an acceptable physical size and physical impairments (such as splitter losses and cross-talk) depending by the exploited modulation format. The level of granularity and the system architecture are determining factors in the number of required switching modules and the number of sub-components in each switching module.

In this deliverable, the switching node architecture proposed in the PASSION project are explained with special emphasis on *Circuitry and technology matching to the path functionality in the optical node*. Target technology platforms for the implementation of circuits is identified. The details on the circuit implementation of the Photonic switch, the Add switch, Aggregate/disaggregate switch, MCS and the Coherent receivers is presented and evaluated based on the preliminary case study scenario.

1 INTRODUCTION

1.1 BACKGROUND AND MOTIVATION

In the last decade we assisted to a continuous growth of traffic in the transport and metro networks. Presently, the bottleneck is in the processing of huge amount of data constituted by growing number of users, the capacity content that is exchanged and the convergence of Telecom (TLC) and Datacom. Thus the optical TLC systems are constantly growing[1] with the promise to support the increasing bandwidth requirements, quality of service (QoS), flexibility, low power consumption and ultimately low cost, for a sustainable evolution of information and communication technology (ICT) infrastructure. According to major analyst forecasts[2,3], the growth of Metro Networks is one of the drive of this evolution.

Looking at the state of the art, the current transmission devices for the Metro Network are evolving from the traditional approach by proposing new improved modulation schemes or, as alternative, coherent transmission solution, which today are used mainly for Long Haul (LH) transmission and are characterized by high cost and high power consumption. Nonetheless, performance such as throughput is only increased by a maximum of 4 times, which is not adequate for network requirements due to traffic increase, e.g. due to 5G and beyond services.

In line with ICT-30 call, the PASSION project aims to meet the above-mentioned requirements by providing innovative solutions covering, *technology*, *architectural vision* and *network management (NM)* tool aspects. PASSION introduces new photonic technologies and devices for supporting agile metro networks, capable of enabling target capacities of Tb/s per channel, 100 Tb/s per link and Pb/s per node over increased transport distances in the range of few hundreds of kms.

The modularity and programmability (via Software defined networks: SDN) system and subsystem components is used to achieve the flexibility demanded by dynamic traffic, channel bandwidth/ path/state/energy requirements of the metro network. A figure showing PASSION metro network with the envisioned infrastructure is shown in Figure 1. The array of modules of sliceable bandwidth variable transmitters (S-BVTx) is based on high-speed, low-energy consumption, high-reliability and low-cost VCSELs, emitting in the C-band. Development of energy-efficient and small-footprint switching technologies for a node featuring functional aggregation/disaggregation, together with switching in the space and wavelength domain will be used to handle high capacity up to 1 Pb/s.

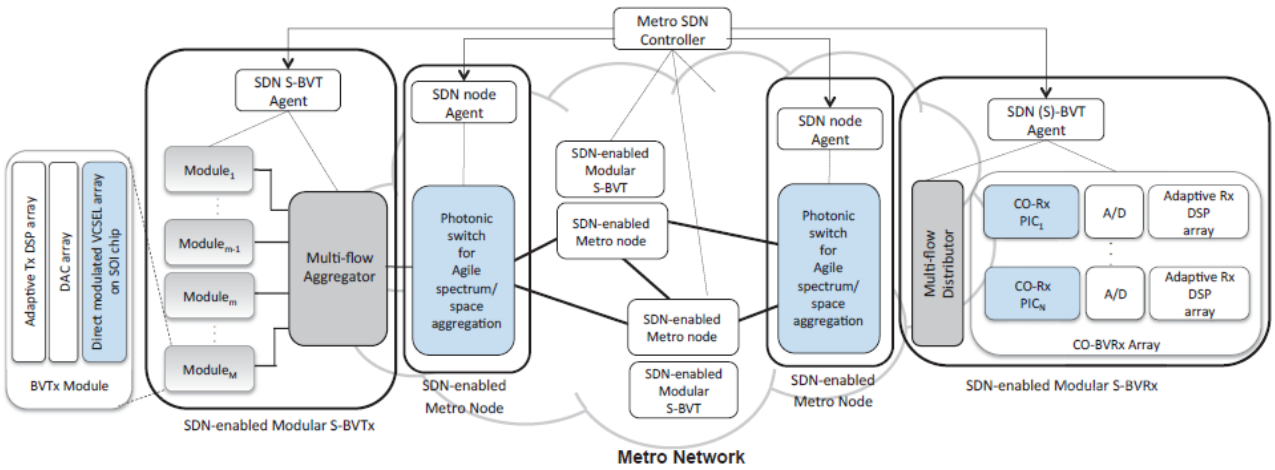

Figure 1. PASSION metro network: envisioned infrastructure, supported by new device technology developments

1.2 NETWORK CHARACTERISTICS

In the PASSION project, a set of target network characteristics are defined to fulfill the requirement of the metro networks by developing novel devices and technologies. They are enlisted as follows:

i. *Reduced network cost, energy/power consumption and equipment foot print*, that are achieved by the development of compact/cost effective switching technologies and transmitters (using direct modulated vertical-cavity surface-emitting lasers, VCSELs) and receiver modules based on Indium Phosphide (InP) technology and dense photonic integration;

ii. *Increased system flexibility* and *modularity* by the adoption of sliceable bandwidth/bitrate variable transmitters (S-BVTs) with reconfigurable parameters;

iii. *Increased network* and *system scalability*, *programmability*, and *re-configurability* that are enabled by agile aggregation in the spectrum, polarization and space dimensions and implementation of SDN control platforms.

1.3 TARGET OBJECTIVES

The main goal of PASSION project is the development of application driven photonic technologies supporting innovative transceivers and optical nodes featuring different levels of aggregation (in spectrum, and space) for an envisaged network architecture able to match the growing traffic demand in the metro connections. The proposed approach is capable of establishing high capacity connection for metro network distances (typical few hundreds of km) with high throughput, low-cost, energy-efficient and reduced footprint devices for massive deployment. End-to-end connectivity for novel services and businesses is achieved with dynamic SDN control of the different systems and subsystems to ensure metro connectivity and deployment of services.

As the optical node and receiver are concerned the PASSION project has defined a set of target objectives enlisted below:

1. Design and development of photonic technologies for the realization of a new generation of compact and flexible receiver (Rx) modules for the metro network able to sustain the PASSION sliceable bandwidth/bit rate approach.

2. Development of energy-efficient and small-footprint switches technologies for a node featuring functional aggregation/disaggregation together with switching in space and wavelength domain in order to handle 1 Pb/s capacity. The optical switching node will enable different levels of aggregation both in spectrum and space in order to effectively leverage the available traffic pipes in an agile manner. Compact wavelength selective switches (WSS) with low electrode number, high connectivity WDM and Multi-cast switches (MCS) with low insertion loss will be designed. Both monolithic and hybrid approaches of the switching node design will be employed.

3. Development of scalable and modular metro network architecture for subsystem sharing and functional reuse to support flexible agile spectrum/spatial switching addressing capacities of Pb/s per node. Based on the integration of all PASSION subsystems via SDN control, proof of the overall system concept will be realized to provide a roadmap for the migration towards future agile high capacity metro networks.

1.4 PASSION PRELIMINARY USE CASES

Target network characteristics are set to define the network framework for the PASSION optical node, based on preliminary use cases, e.g. support of dynamic traffic originating from a future 5G scenario, which will likely be the most challenging for the switching operation. Initial network and system use cases have been analyzed in details in the WP2 task T2.1 (milestone MS1). The PASSION optical node is able to support the dynamic network at two levels: Metro-access scenario and Metro-core scenario. In the metro access network two distinctions are made for optical front haul and optical backhaul structures in which the PASSION switching node can be used.

As for the features and performance specifications for 5G, the key performance parameters of eMBB (enhanced Mobile Broadband), mMTC (massive Machine Type Communications) and URLLC (Ultra-Reliable and Low Latency Communications) are the peak data rate, latency and connection density. This is possible via the cloudification of 5G Core Networks and RAN (Radio Access Network) giving more distributed network functions for satisfying all the uses cases.

1.4.1 Metro-Access Scenario: Dynamic fronthaul

Mobile front-haul based on the CPRI (Common Public Radio Interface) is the most bandwidth hungry service as indicated by high data consumption. Looking into cell load information, we need more bandwidth elasticity in 5G more than ever. Following this main idea the capacity for dynamic bandwidth provisioning is presented in the fronthaul architecture composed by a 5G edge connected with the exchange nodes in the Metro/Aggregation site and connected with several BVT (Bandwidth variable Transponder) and ONUs (Optical Network Units) in the Access site by the aggregation point following a Tree/urban topology.

Figure 2. shows the basic topology structures of the optical front-haul. The point-to-point (PTP) where there is a based band unit (BBU) host in a central site with direct connections to the RRH (remote sites). The tree PTP where there is also a BBU in the central site connected with several aggregation points in local sites and each one connected to the RRH. By last, the double ring topology architecture where the central site BBU host is connected to several aggregation points connected between them at the same time and also each one connected to the local site RRH. In the topology comparison the most cost-effective architecture are Tree/urban and Double Ring/Urban topologies.

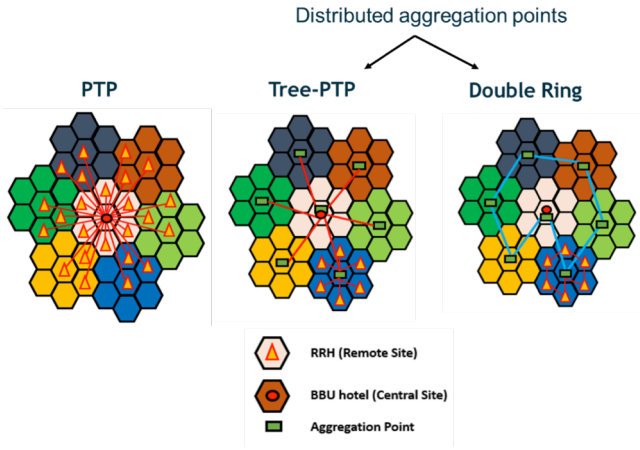

Figure 2. Basic topology structures for the optical fronthaul

1.4.1.1 Sample backhaul scenario

To show the sample 5G backhaul scenarios, three routers types have been presented with different characteristics as shown in Figure 3(a). The Metro-Core Node in the hub of the region, multiplexes channels from input ports to sliceable-BVT (S-BVT) port with 1000 Gb interfaces. The Metro-Regional Node in the regional mesh, multiplexes to/from S-BVT port with 400G interfaces. By last in the very low level (ring) the Metro-Access Node multiplexing of mx10GE client signals into an nx10G flex channel. For one approach with no PON support shown in Figure 3. (b), the PASSION metro-regional node are connected by S-BVT to BVT with the PASSION metro-Access Node and by TWDM-PON OLT connected to different areas (Business Area, Sports Area) without any priority.

On the other hand, the second approach integrating PON support (Figure 3. (c) and (d), the PASSION metro-Access Node with S-BVT-PON creates different P2P flexgrid channels giving priority to one area (shown in blue and purple channels) while the yellow is a shared channel used for basic connectivity. For example, for the sport area during the game (Figure 3. (d)) flexi-grid channels are sent to the stadium while giving shared PON channel for basic connectivity to the rest of the areas.

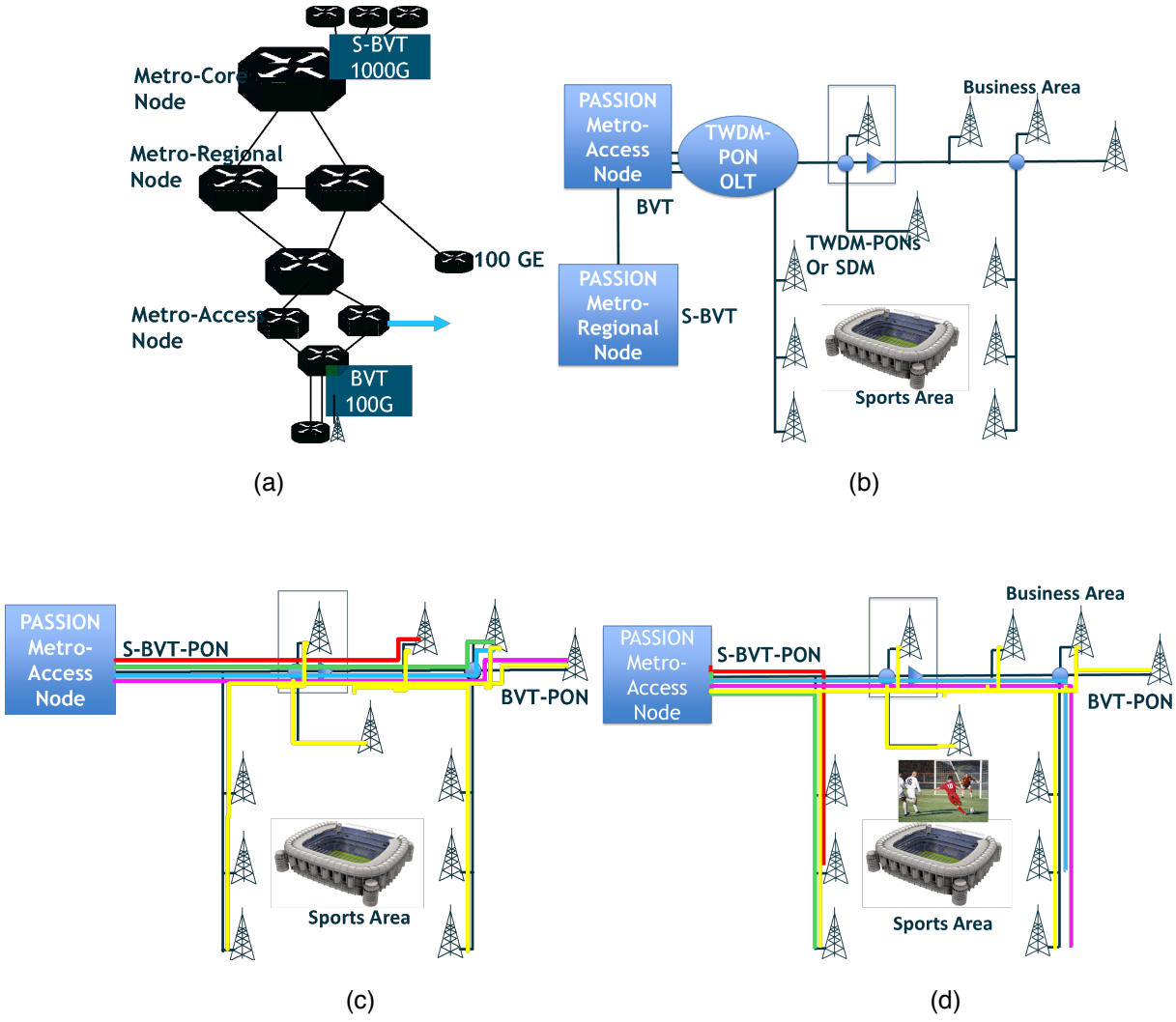

Figure 3. (a) 3 types of Metro nodes (b) sample 5G backhaul scenario no PON support (c) integrated PON support before the game (d) integrated PON support during the game.

1.4.2 Metro-Core Scenario: Multiflow configuration capabilities

In metro core scenario, multi-flow configuration is enhanced by optical paths between central and distributed data centers which employ statistical multiplexing of the S-BVT.

1.4.2.1 NFVI

A Network Functions Virtualization Infrastructure (NFVI) could be defined for a several standards for compute and storage resources to build Virtualized Networks Functions (NFV) as a key concept inside the NFV architecture where the hardware and software components for the virtualization of the network are present.

The NFVI standards increase the interoperability of such components of the networks and give the capacity to enhanced multi-domain environments.

Deployment of computing facilities across operator's networks brings the opportunity of offering part of such infrastructure to third parties to create multi-domain networks and thus is foreseen to take place by means of open interfaces. Such interface leads with the different services as the broadband access in dense areas, highly user mobility, massive internet of things, etc. to offer by the network applications (Business, Mobility, Video, Consumer and Cloud). To give support to those services applications it is necessary to configure the whole components of the networks as central data center (DC), regional data center (DC), Cloud POP (Point Of Presence) and vBranch. This supports the main objective of delivering content from servers located in Centralized Data Centers to end users.

1.4.2.2 Cache Backup and Sliceable BVT

As the traffic nature is dynamic (events in stadiums during the game, popular contents in regions, etc.), the option is to deploy a Virtualized network function infrastructure (VNFI). The VNFI has the same capabilities as current deployments, but its provider can dynamically activate virtual machines in locations that require more content servers e.g. from a big-town as usual requirements but also from a small-town in some eventual cases. Once the server is activated, the contents can be transferred from a national/regional data center to sync the most popular content.

This requires locating the access node connected with the distributed data center in each location and establishing a great communication between them with several restoration paths to provide cache backups and get the nearest cache depending on the needs. The access to these cache backups can be done in different ways in order to improve the shared protection in a distributed DC scenario. It can also be changed dynamically to obtain this content from the Centralized protection server located in the Capital CO (central office).

This transmission between central and distributed DC will be deployed by optical paths with statistical multiplexing efficiency by using S-BVT (Sliceable-Bandwidth Variable Transponder). This S-BVT would be a key building block to enable cost-effective EON (Elastic optical network) in a NFVI due that a Sliceable Bandwidth Variable Transponders can be sliced into several virtual transponders at different bit rate and to different destinations when the optical spectrum will be completely consumed by 2020.

2 PASSION OPTICAL NODE ARCHITECTURE

2.1 CAPACITY AND GRANULARITY

Aggregation of channels in spectrum and space are well known to modularly upgrade transmission capacity and increase system flexibility. A spectral superchannel is an aggregation of signals conveyed on adjacent carrier frequencies. A multi-core fiber (MCF) allows increasing the transmission capacity carried by a single fiber by aggregation of signals conveyed in multiple cores.

One of the main objectives of PASSION project is the development and deployment of fundamental photonic technologies to support agile metro networks, capable of enabling target capacities of Tb/s per channel, 100 Tb/s per link and Pb/s per node over increased transport distances according to the network operator requirements and roadmaps based on spectral and spatial super channels. PASSION's goal is achieved by exploiting VCSEL sources, each one operating at a different WDM channels in the C-band, directly modulated to obtain up to 50 Gb/s rate to target up to 8-Tb/s capacity at a single polarization. 16 Tb/s per

spatial channel are achieved exploiting polarization-division multiplexing, while the spatial dimension of 7 cores MCF or 7 fibers in a bundle allows enabling up to 112 Tb/s aggregated capacity per link.

This objective is pursued with a modular approach as shown in Figure 4. i.e. at the transmitter 40-VCSEL based modules (each sub-Module in the green box contains 10 VCSELs) are built covering the entire C-band with 100 GHz granularity (with 2 Tb/s capacity), that can be fine-tuned by 0-75-GHz with current or temperature. By combining four of such a module (shown in red box) with external inter-leavers a full 160-ch Tx module (8 Tb/s capacity) is built with 25-GHz granularity. This type of modularity offers the ability to fabricate and stock only one module type, and to use the identical 40-ch modules (shown in red boxes) to build the full 160-ch Tx super-module (shown in yellow box). Then, a discrete polarization multiplexer combines inputs from two identical 160-ch Tx modules to get 16 Tb/s capacity. Finally, signals are coupled to multi-core fibers or fiber ribbons using spatial multiplexers for the fully equipped S-BVT.

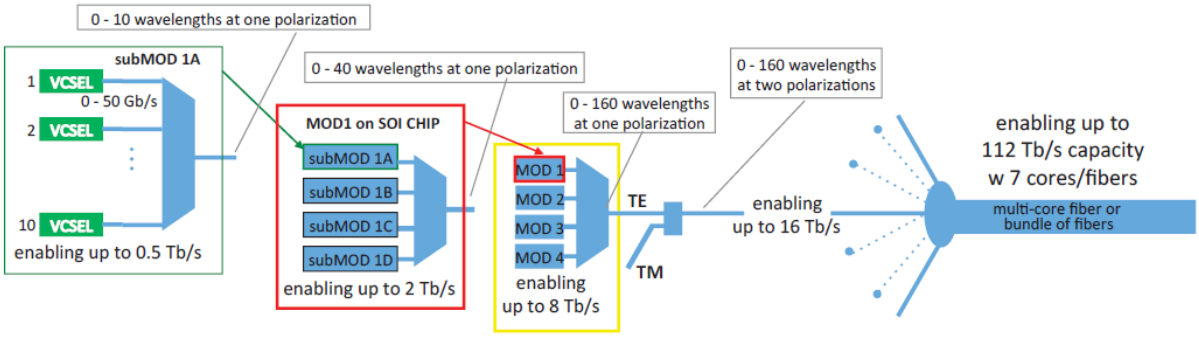

Figure 4. Example of Tx module capacity aggregation exploiting the spectral and space dimensions

2.2 SWITCHING NODE FUNCTIONALITIES

In this section, the switching node functionalities as demanded in flexible reconfigurable add and drop multiplexer (ROADM) is explained. The Add/drop, aggregate/disaggregate functionalities and optical inter - connection via spaced switching will be used together. Being able to switch any input-to-any output provides *colorless* and *directionless* performance. The *contentionless* performance can be achieved by combining photonic space switching functionality with wavelength selective and multi-cast switching functionalities. The use of multicast switches (MCS) along with coherent reception provides color-less, direction-less and contention-less (CDC) performance. These functionalities will be greatly helpful adding configurability and flexibility and removing the constraints of costly manual intervention.

PASSION system architecture: current state-of-the-art metro networks are quite static and present limited flexibility and scalability. The optical node architecture in the PASSION project will be a key enabler of network flexibility and agility required to address cost and efficiency requirements. The switching node functionalities described in section 2.2 will be employed to enable dynamic switching on spectral domain to flexibly accommodate the agile and high capacity requirement within the metro-core nodes. This metro network concept will leverage modularity and exploits the SDN (software defined network) paradigm in order to efficiently allocate/use the overall network resources transforming the operation of todays network infrastructure and reducing overprovisioning and margins.

Figure 5. shows the architecture of an optical switching node in the PASSION project. At the heart of the PASSION node is the photonic switch providing connectivity between the express and add/drop traffic. It consists of BVTs with capacity to variably allocate bandwidth, optical switching components for handling *express traffic*, *added traffic* and *dropped traffic and coherent receiver modules (CRMs)*. The BVTs are used to transmit the locally generated traffic at that particular node. The locally generated traffic and aggregated traffic are merged as *added traffic*. The switching functionality is implemented via *photonic switches*, *add switches*, *aggregate/disaggregate switches*, and *multicast switches (MCS).* The system capacity is enhanced

by using the space, spectrum and polarization dimensions. The spectral diversity is enabled via WDM inputs and outputs, while the space diversity is enabled with multi- core fiber inputs and outputs as explained in Section 2.1.

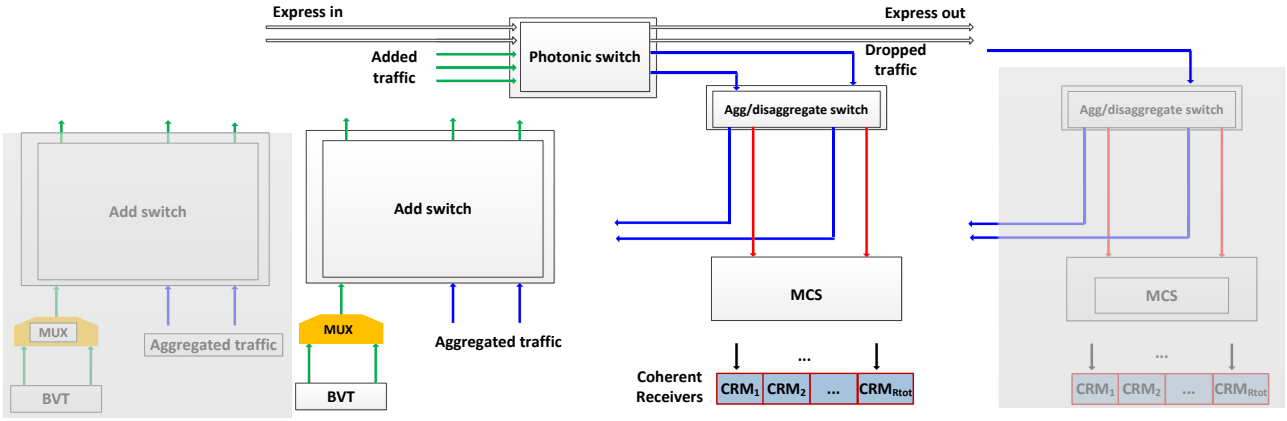

Figure 5. Optical node architecture, with sub-component functionality (BVT: bandwidth variable transmitter, MCS: multi-cast switches, CRM: coherent receiver modules)

The *Photonic switch* provides higher level switching of the traffic at any input port to any output port which are either assigned to *express out* path or *dropped traffic* path. A high level of flexibility is needed to be able to fully reconfigure the data traffic, while being able to add/drop on the fly and guarantee full link usage at the same time. This is done by including spectral slicing, space switching, and merging and aggregation functionalities. The Aggregate/disaggregate switches do the routing of the dropped traffic either to the MCS switch or Add switch on the level of wavelength granularity. The Add switch provides merging and aggregating tasks for the WDM inputs originating from BVTs or from the aggregate/disaggregate switch to the add ports of the photonic switch. In this way, the available transmission resources are efficiently used. The capability of the BVT to generate traffic with variable bandwidth based on the granularity principle given in Section 2.1 meets the agile capacity requirement of the nodes. Add ports of the photonic switch allow to flexibly add each of the requested channels.

The drop part diverts some of the link traffic to drop it at the receiver side. For this purpose, the Multicast switches (MCS) enable colorless and contentionless switching to efficiently use the available coherent receiver modules (CRMs). Each CRM contains *M* coherent receiver modules each of which is equipped with its own local oscillator, and the total number of receivers is $M \times R_{tot}$. The main motivation behind this presented architecture is the bundling of traffic in space and wavelength dimension to efficiently utilize resources. When the node needs capacity upgrade, the same blocks are repeated (as shown in the shaded blocks in Figure 5.) as a result of the flexible and modular design of the node architecture.

In the next subsections, a brief description of these switching functionalities as presented in Figure 5., i.e. photonic space switching, adding and dropping, aggregation/disaggregation, coherent detection is given.

2.2.1 Photonic space switching functionality

The use of high port count inter-connectivity functionality generated by the photonic space switching is important to provide non-blocking switching between the express traffic and the add/drop traffic. It sends the express traffic through the node towards the next destination nodes. In the presence of high capacity at the node (i.e. several wavelengths per port and large port counts) switching at wavelength granularity creates switching complexity which is solved by photonic space switching which does switching wavelength bundles. In PASSION project, control information from an SDN agent provides switching information between the express line traffic and the add/drop traffic. This will reduce the system cost as less switching components

are required by avoiding wavelength granularity at this core switching stage. The wavelength selective features are implemented to the Add/drop and Aggregate/disaggregate functionalities.

Since the photonic space performs central switching functionality, it presents a single point-of-failure in the metro-core scenario. The solution to this is the use of identical core photonic space switch for the protection purposes. To support scalability, the design of the photonic space switch targets a low-cost and large port count implementation.

2.2.2 Adding and dropping switch functionality

The add/drop functionalities provide connectivity by adding to or dropping from the express traffic at the local optical node. In support of greater operational flexibility, and with the advent of wavelength-tunable transceivers, the wavelength selective switch (WSS) is a popular choice for “colorless” add/ drop ports. In a 1×N WSS configuration, wavelengths can be routed from any input of the network node to any output fiber, or channels can be locally dropped.

In order to enable direction-less performance reachability of a wavelength from any input to any output port is fulfilled via M×N WSS so that dropped/added to any desired direction is possible. The contentionless attribute is enabled via the use of multi-cast switches (MCS) in the drop direction in which the signals at the input ports are broadcast to all output ports irrespective of the wavelength, and the use of space switches at each MCS output port to generate contention free performance.

In PASSION, scalability to high capacity in the add and drop functionality supports the use of modular approach where new add/drop modules are used to support new subscribers as shown in Figure 5.

2.2.3 Aggregation/Disaggregation switch

The benefits of spectral super-channels for high-throughput transmission, system component integration, and reduction in the number of switching components have been widely studied and demonstrated. MCF have been of interest recently, and their benefits for increasing per-fiber throughput and enabling system component integration has been demonstrated.

As the bit rates of routed data streams exceed the throughput of a single WDM channel, spectral and spatial traffic aggregation become essential for optical network scaling. These aggregation techniques reduce network routing complexity by increasing spectral efficiency to decrease the number of fibers, and by increasing switching granularity to decrease the number of components in a photonic switch matrix. Spectral aggregation yields a modest decrease in the number of fibers but a substantial decrease in the number of switching components.

To derive maximum benefit from the optical node transceivers, it is desired that they are “directionless,” and hence able to serve drop (add) channels arriving from (directed to) any network link connected to the node. In PASSION, we aim to achieved this by adding additional hardware (aggregate/disaggregate switch) that serves to aggregate the directions and distribute the add/drop channels to the available transceivers. To achieve scalable performance of the aggregate/disaggregate switch, it is recommended is to use a modular WSS.

2.2.4 Multicast switch

To achieve a CDC performance the aggregate/disaggregate switch functionality is supported by a MCS solution for the drop wavelength channels.

A MCS splits the drop signals and delivers a copy of all the drop channels to each attached receiver. The embedded function of a tunable wavelength filter in the modular WSS employed in the MCS isolates a single drop channel from the selected direction and thus implement contentionless operation of the node. In principle the coherent detectors with tunable local oscillator can also be used for this purpose. However, pre-

selecting the channel to be dropped improves the coherent detection system by avoiding saturation of the coherent detector, resulting in higher sensitivity.

2.2.5 Coherent detection

Coherent detection offers several key advantages over direct detection i.e. greatly improves receiver sensitivity, achieves much higher capacity in the same spectral bandwidth, can be used to compensate for fiber impairments with the aid of digital signal processing (DSP), increase signal-to-noise ratio with balanced detectors and replace tunable filters for agile wavelength selection by tuning the local oscillators. In PASSION project, we will take advantage of these coherent detection scheme, revisiting it in a modular fashion, for offering high bandwidth and low power consumption detection.

In the context of metro networks, coherent detection implementation needs to be highly efficient in terms of cost and energy. These are among the main drivers in the coherent receiver module development (CRM) within PASSION. Today's multi-channel InP coherent receiver (CO-Rx) architectures are monolithically implemented and accept two polarisation de-multiplexed inputs (TE and TM) edge-coupled from the facet through bulk optics in the module. The two polarisation components are first split and then the TM component is rotated so that all light in the PIC itself is TE-polarised[4]. These architectures have been designed and fabricated to be used in high-cost, high- performance, long-haul transmission DSP-assisted systems.

Shorter transmissions systems such as those envisaged in PASSION demand lower-cost, good-enough performing devices. EFP's low-cost, non-hermetic packaging technology will be leveraged in the realization of the coherent receivers. Unlike the current technology, we aim to implement polarisation handling on chip, such that only a single fibre coupling is needed on the CO-Rx, and hence the packaging can be greatly simplified. The coherent receiver also targets to incorporate in the same PIC a narrow linewidth, widely tuneable, etalon-free laser to server as local oscillator. The concept of this CRM implementation is shown in Figure 6. A set of *M* WDM signals carried in *M* optical fibers are received at the module. The CRM consists of *M* submodules, each representing a dual polarization coherent receiver. The figure below also shows the architecture of the submodule.

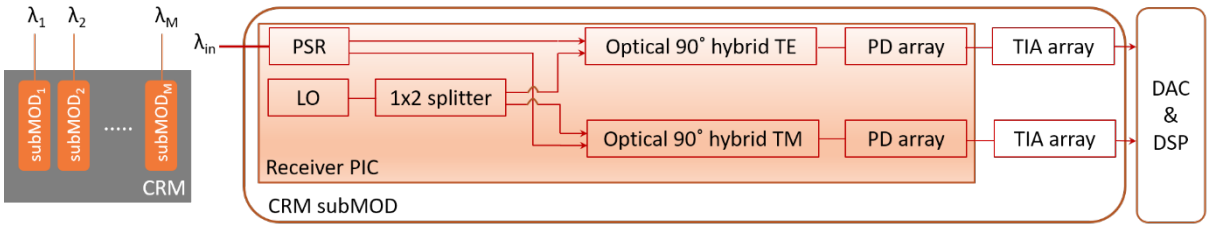

Figure 6. Representation of the modular, scalable dual polarization coherent receiver. Left: coherent receiver module (CRM) consisting of M submodules, each representing a dual polarization coherent receiver. Right: submodule architecture. PSR: polarization split

This innovation also impacts positively the packaging and hence the cost. Moreover, a more than 25 GHz detection bandwidth will be offered to comply with the requirements of the transmitted data. The integration approach for the CRM is to be determined considering the best trade-off in cost, power, and footprint, and to satisfy the flexibility, and the 'pay-as-you-grow' character demanded by the network.

2.3 KEY SYSTEM PARAMETERS OF THE OPTICAL SWITCHING NODE

In this section the key parameters of the optical switching node are briefly described. It is important to monitor and optimize these parameters during the implementation stage as different design choices affect these system parameters uniquely.

Power Consumption: Power-efficiency is key performance criteria for reducing the energy-related costs of the optical node. The power consumption of a WSS modules increases with the number of wavelengths and the number of input/output ports. With increased input/output ports the increased splitter losses have to be compensated by a single or cascaded booster amplifiers which also contributes to the overall power consumption. Design of the optical switching node to minimize the number of power-driven components such as the SOAs and technology choice to minimize the coupling losses is a key target implementation requirement.

Cross-talk: Crosstalk is caused by undesired signal originating from poor/limited isolation of the various component blocks cascaded in the switch. The generated cross-talk can be *interferometric* i.e. it is caused by unwanted channels at the same wavelength as the wanted channel or *inter-channel crosstalk* i.e. it is caused by disturbing channels at wavelengths different from that of wanted channel. The total cross-talk in the switch path is the power of the accumulated signal level from all unwanted channels. Poor extinction ratio in switching gates and inter-channel cross-talk in among AWGs channels in the WSS contribute to the overall cross-talk. The target cross-talk level for the switching functionalities presented in Section. 2.2 is given in Section 3.

Optical-signal-to-noise ratio (OSNR): Maintaining the optical signal to noise ratio (OSNR) to an acceptable level is important for the correct demodulation of the information to the end users. The OSNR penalty in the optical switching nodes comes from noise contribution of a number of booster (single or cascaded) amplifiers implemented within *Add switches* and *MCS*. Other factors contributing at the OSNR penalty is undesired pass-band roll-off (increased pass-band loss) in wavelength channels of AWGs used in WSS modules.

Form factor and cost: With increasing capacity requirement, the size of the optical switching node along with Capital Expenditure (CapEx) and Operational Expenditure (OpEx) cost are crucial in the practical deployment. In PASSION project we adopt photonic integration to reduce form factor by implementing all the functionalities in a compact PICs and the cost reduction can be attained by reducing energy related costs.

3 CIRCUITRY AND TECHNOLOGY MATCHING TO THE PATH FUNCTIONALITY IN THE OPTICAL NODE

Figure 7. shows the PASSION optical switching node architecture with proposed embedded sub-component architectures.

In the proposed circuit implementation, the following design choices are made:

- The photonic switch is implemented as a space switch
- The aggregate/disaggregate switches makes use of 1×2 WSS per input port to route the traffic for either aggregation or disaggregation (i.e. either to the Add switch or to the MCS)
- The Add switch will consist of broadcast and wavelength select network consisting of power splitters (PS) and WSSs

Furthermore, the following technology matching is made:

- The photonic switch will be implemented in a polymer PLC technology due to its low-cost, low-loss features, and low power consumption while supporting large number of ports.
- The aggregate/disaggregate and add switches are implemented in InP technology and later will be integrated on SiPh interposer for low-loss coupling
- MCS will be implemented in InP platform which will then be integrated on SiPh interposer for loss-less coupling.

***Case study definition**: in evaluating the proposed building block circuitry presented in this section, a use case scenario is defined in which the optical node attains a capacity of **2 Tb/s** per port via the use of **40 wavelengths**, each of which is **100 GHz** apart, with 50 % drop ratio. The number of input output ports for the photonic switch is $M_{ph}=N_{ph}=16$ (leading to a node capacity of 32 Tb/s, for the aggregate/disaggregate switch is $M_{agg}=8$, $N_{agg}=16$, for the MCS is $M_{MCS}=8$, $N_{MCS}=16$, for the Add switch is $M_{add}=10$, $N_{add}=8$.*

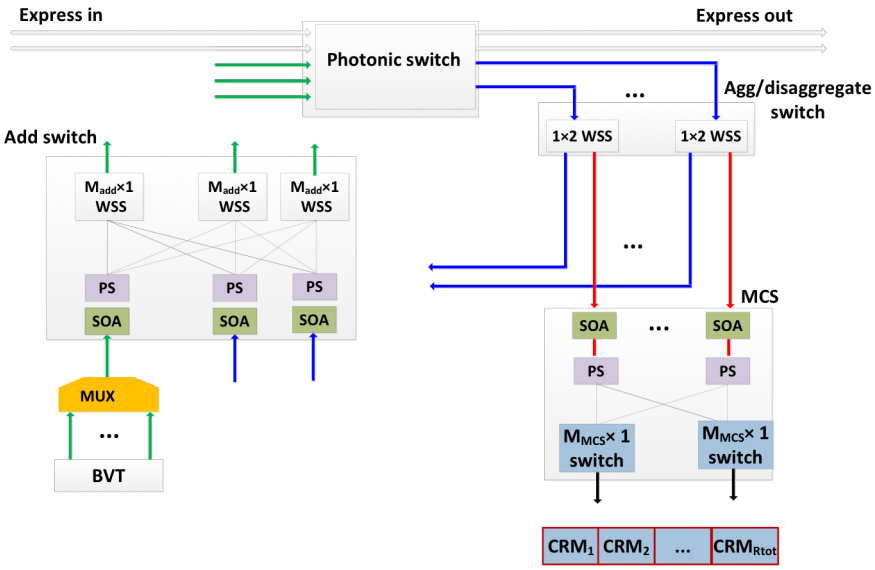

Figure 7. Optical node architecture, with subcomponent functionality, BVT (bandwidth variable transmitters), PS (power splitters), Photonic space switch, WSS (Wavelength Selective Switch), MCS (multi-cast switch), CRM (Coherent Receiver Module)

The proposed architecture for each of the subcomponents is explained in detail in the next sections.

3.1 Photonic Space Switch Parameters and Architecture

The photonic switch has M_{ph} input ports and N_{ph} output ports. Out of the input ports, A_d ports are the designated add ports, while out of the output ports, D of them are designated drop ports, i.e. $N_{ph}=D+P_{thr}$ and $M_{ph}=A_d+P_{inc}$.

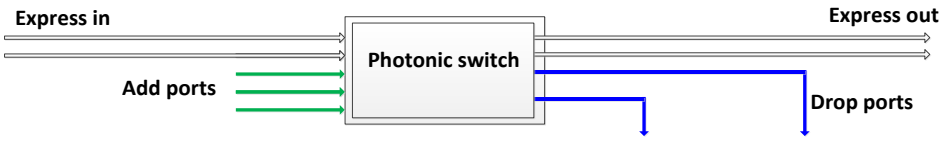

Figure 8. Photonic switch functionality implementation via planar PLC technology

Switch parameters	Symbol
Total number of input ports	M_{ph}
Total number of output ports	N_{ph}
Total number of ports for dropped traffic	D
Total number of ports for outgoing traffic	P_{thr}
Total number of ports for incoming traffic	P_{inc}
Total number of ports for added traffic	A_d
Percentage of input ports for added traffic	***a %***
Percentage of input ports for dropped traffic	**d %**

Table 1. Parameters of the photonic switch

The percentage of output ports ***d %*** assigned to the dropped traffic out of the total number of output ports in the *photonic switch* is fully dependent on the traffic capacity demand at the particular node. The same condition applies for the choice of the percentage of input ports assigned for the added traffic ***a %***.

Photonic Switch Implementation in Polymer PLC: The photonic switch (optical switch matrix) to be developed in PASSION project employs the polymer-based integrated planar lightwave circuit (iPLC) technology. There have been several approaches to implement an optical switch matrix [5-10]. Among them, the switches based on 2D (or 3D) micro-electro-mechanical system (MEMS) technology showed the best performance. However, the switches based on MEMS are too complicated to be implemented in low-cost mass production. Because of that, an iPLC technology based on the silica or polymer material has been considered as a promising candidate for the optical switch matrix with the advantages of easy packaging, mass productivity, non-moving part, long-term reliability[7-14]. In a silica-based optical switch matrix, it has a very low-loss characteristic, but is usually operated by phase control and thus sensitive to wavelength and polarization changes. Furthermore, these types of silica optical switch matrices are too much complex in structure to overcome the silica's poor switching properties due to their high power consumption resulting from the low thermo-optic coefficient of the material and are quite big in size. Therefore, polymer-based optical switches have been preferable to overcome the above-mentioned issues[9-15]. The PASSION photonic switch will be comprised of a polymer thermo-optic 1x2 the total internal reflection (TIR) switch as a switching element, which has an asymmetric Y-branch of multimode polymer waveguides and a heater electrode to induce the TIR by the thermo-optic effect on the branched node, shown in Figure 9(a). When the electrode is heated up the refractive index of the polymer near the heater is decreased to cause TIR. A conceptual schematic configuration of optical switch matrix (photonic switch) with inputs designated as I-1, I-2, …, I-N and outputs designated as O-1, O-2, …, O-N is illustrated in Figure 9(b). The individual switching element is constituted with single-mode input/output ports, tapered waveguide region for mode conversion, and switching node with branched multi-mode waveguides. To form the switch matrix, the straight multimode waveguides are crossed each other at a shallow angle which is corresponding to half the branched angle of the switching element. The heater electrodes to induce TIR are formed on each crossed node or branched node on the edge side of the switch. The location of the heater is offset toward the upper side of the cross point to improve the internal reflection efficiency, considering the shift of the reflective interference by the thermal diffusion.

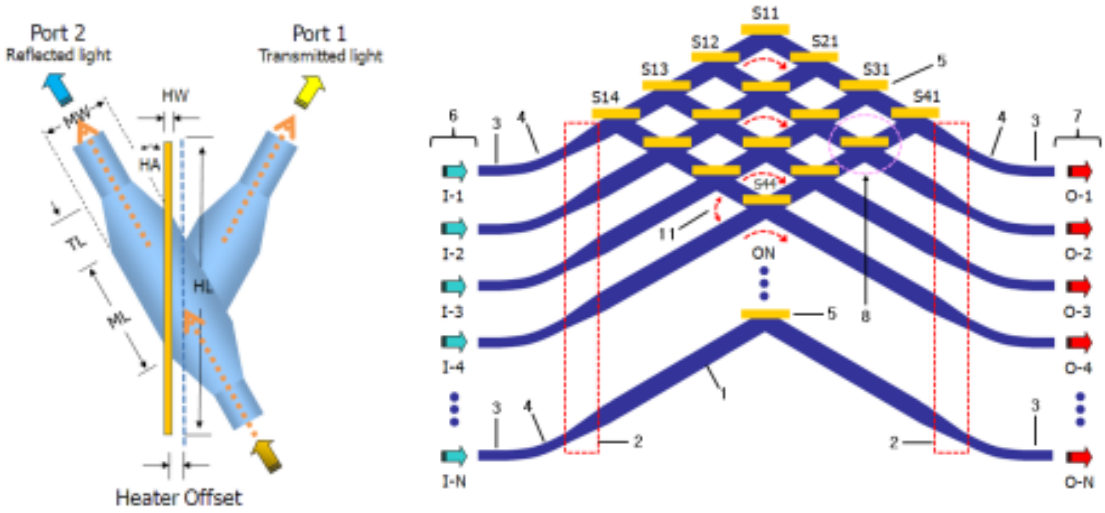

Figure 9. (a) TIR switching element, (b) NxN optical matrix switch

The principle of switching operation is as follows; if the light is injected into the input ports of the single-mode waveguide, the light is adiabatically expanded in the tapered region to a 0th-order mode (fundamental mode) of the multimode waveguide and then it propagates through the multimode waveguide. At a crossed (or branched) node, if the electrode is turned-off, the light passes straight. Otherwise, the light is reflected into the crossed waveguide by TIR induced by the decrease of the reflective index. Through the combination of the on/off setting at the switch electrodes, each injected light will be routed to the corresponding output ports, which allows non-blocking switching. Table 2. shows the target specification of the implementation of an optical switch matrix.

	Unit	Target
Operational band	-	C & L
Insertion loss (max)	dB	< 6.5
Loss uniformity	dB	< 1
PDL	dB	< 0.5
Extinction ratio (min)	dB	> 45
Switching time	ms	< 3
Port number	-	16x16

Table 2. Target specification of polymer-based optical matrix switch.

Case study evaluation: For the considered M_{ph}=N_{ph}=16 input/output ports, the number of required electrodes is $N_{ph}2$= 256. The power consumption per switch element is 30 mW.

3.2 AGGREGATE/DISAGGREGATE SWITCH: PARAMETERS AND ARCHITECTURE

The schematic representation of the Aggregate/disaggregate switch is shown in Figure 10. The Aggregate/ disaggregate switch separates wavelengths to be aggregated and dropped to outgoing to express traffic to the Add switch and to MCS, respectively as described in section 2.2. The number of input ports is $\mathbf{M_{agg}}$ and the number of output ports is $\mathbf{N_{agg}}$. Each port is equipped with a **1×2 WSS**. As a result, the number of output ports $\mathbf{N_{agg}}$ is twice that of the number of input ports $\mathbf{M_{agg}}$. By duplicating the number of input ports at the

output, wavelength contention is avoided at the aggregate/disaggregate switch port. In this proposed architecture a total of **M_{agg} 1×2 WSS** are used.

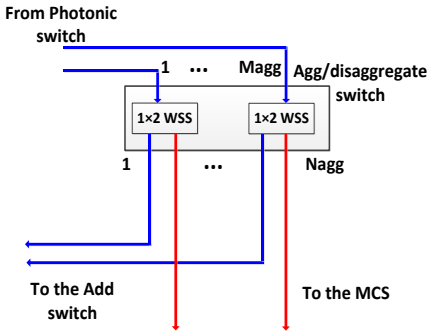

Figure 10. Schematic of aggregate/disaggregate switch

1 × 2 WSS: The purpose of a **1×2 WSS** switch is to provide colorless, directionless and contentionless (CDC) routing performance of the dropped traffic either to the **Add switch** or the **MCS switch**. As such two possible architectures of a **1×2 WSS** implementations (shown in Figure 11. (a): option-1 and Figure 11. (b): option-2) are considered.

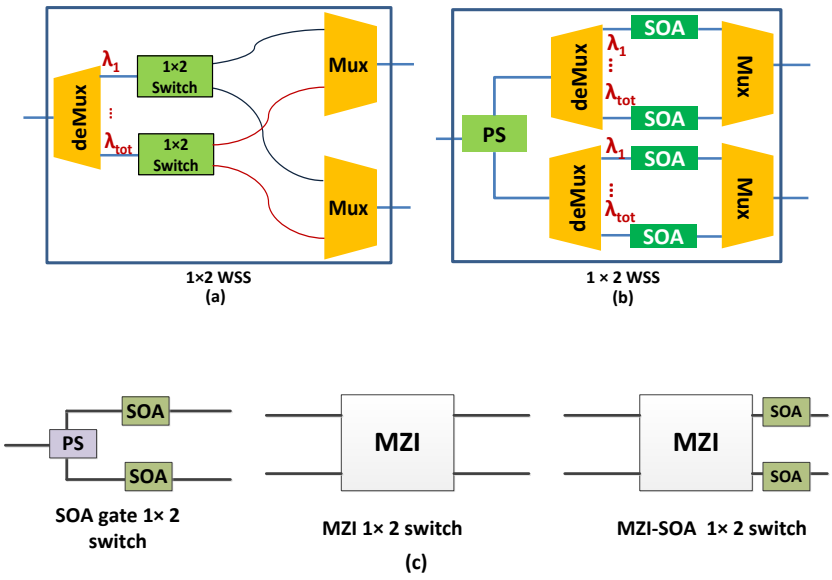

Figure 11. Schematic representation of a 1×2 WSS (a) Option-1 (b) Option-2 (c) implementation Option-2 of 1×2 switches

The two presented configurations are compared based on the number of required components (directly related with the device footprint), the power consumption and losses related with the power splitters (**PS**) and the number of cross-overs, and device foot print. The implementation given in Figure 11. (a) employs a 1×2 WSS which makes use of 2 Mux structures, and 1 deMux structure. The complexity of the deMux/Mux structures, the required number of 1×2 switch gates and the number of cross-overs increases with the total number of wavelengths **λ_{tot}.** The 1×2 switches can be implemented either via SOA gate switches or MZIs switches. The large absorption of the SOAs on the OFF state and gain in the ON state results in enhanced extinction ratio. Moreover, the gain from ON state of the SOA is able to compensate the optical losses of the deMux and Mux.

Hardware cost of a 1 ×2 WSS	Option-1	Option-2
Number of deMux/Mux	3	4
Number of 1×2 MZI switches	40	NA
Number of SOAs	-NA for MZI switches -80 short gain SOA (40 active at a time) for hybrid-MZI switches	80 but only 40 active at a time
Power consumption	8*(40*$\mathbf{P_{MZI\text{-}SOA}}$ +40*$\mathbf{P_{MZI}}$)	8*40*$\mathbf{P_{SOA}}$ (because 40 SOAs are active at a time)
Cross-talk level	For MZI: -20 dB [18,19] MZI-SOA: -50 dB[17]	- 70 dB[16]
Estimated switch size for M_{agg}=8, N_{agg}=16	- incurs additional foot print due to 8×40 MZIs	- incurs additional foot print of 8 AWGs
Number of cross-overs	- More than 40 cross-overs - 0.05 dB[20] loss per crossing - Cross-talk (< -35 dB[21])	NA
Gain/loss	-Insertion loss per AWG= 2-4 dB -Gain of short-SOA (450 µm)=15 dB at a bias current of 50 mA -Loss of MZI=1-3 dB	-Insertion loss per AWG= 2-4 dB -Gain of Long SOA (900 µm)= 30 dB at a bias current of 100 mA

Table 3. Comparison of 1× 2 WSS switch architectures for the case study scenario

The implementation given in Figure 11.(b) uses separate demultiplexing and multiplexing structures for the two outputs of the WSS. A separate SOA gate per wavelength is used as a switching element. Figure 10. (c) shows the different options for implementing a 1×2 switch. In the SOA gate switches, two SOA are used as a main switching element in the alternating on/off states. An MZI switch is used as a 1x2 switching element even though it suffers from poor cross-talk. Another option is the use of 1x2 MZI switch with short SOAs at the two outputs in the hybrid MZI-SOA approach. The short SOAs in the MZI-SOAs are used to either compensate the loss on the ON state or enhance the suppress signal on the off-state to achieve lower cross-talk between the two output ports.

Number of required Mux/Demux AWGs: Comparing, the two architectures, we find that additional 1 deMux/MUX **AWG** is required per 1×2 **WSS** (i.e. an additional 1 AWG per input port of Agg/disaggregate switch). The typical insertion loss of the AWG mux/demux is 2-4 dB in InP platform implementation.

Number of required SOAs: The number of required SOAs for gate switching in Option-2 is the same as Option-1.

Power Consumption: Comparing the power consumption of the Aggregate/disaggregate switch architectures we find that switching based on MZI-SOA switches has significantly smaller power consumption as compared to the SOA gate switches[16]. The power consumption of MZI is significantly lower, and by using short SOA, the over all power consumption can be reduced.

Number of waveguide crossings: Each cross-over in InP generates 0.05 dB of optical loss -35 dB cross-talk level per crossing[20,21]. In Option-2 no loss and cross-talk due to cross-overs is incurred.

Estimated footprint: In Option-2, additional foot print of $\mathbf{M_{agg}}$ Mux/Demux AWGs is incurred, while on the other hand, in Option-1 additional footprint of $\mathbf{M_{agg}}$ 1× 2 MZI switches is present.

Crosstalk: The SOA gate switches can suppress the cross-talk down to -70 dB[18,19], while MZI-SOA gates can achieve cross-talk level down to -50 dB[17]. The MZI switches perform the worst in terms of cross-talk reaching levels up to -20 dB.

Case study evaluation: Comparing the two configurations of a 1×2 WSS of Aggregate/disaggregate switch for the case study scenario definition in which 40 wavelengths spanning C-band are considered. The number of input considered input ports M_{agg}=8; and output ports is N_{agg}=16. The number of required Mux/Demux AWGs is 24 and 32 for option-1 and option-2 respectively. The required number of SOAs is 40 short gain SOAs and MZI switches in case of option-1 and 40 longer SOAs in case of option-2. Comparing the gain of the switching paths, option-2 has additional gain more than 10 dB due to the longer SOA gates. Table 3. summarizes the case study evaluation for the two design options.

Looking into the two design options considered, we primarily consider Option-2 for the following reasons. In Option-1, the number of waveguide crossovers increases with the number of inputs and with total number of wavelengths which leads to increased cross-talk and loss. The effort to optimize performance by making 90-degree the cross-overs takes considerable space. Thus, Option-2 is the primary design option.

3.3 ADD SWITCH : PARAMETERS AND ARCHITECTURE

The schematic representation of the Add switch architecture is shown in Figure 12. It has $\mathbf{M_{add}}$ input ports and $\mathbf{N_{add}}$ number of output ports. The total number of wavelengths is $\boldsymbol{\lambda_{tot}}$. The architecture makes use of a power splitter (**PS**), in which all the WDM inputs are broadcast to the output ports. $\mathbf{N_{add}}$ $\mathbf{M_{add}}$ **×1** WSS, each corresponding to each output port are used to merge and selectively add wavelengths to the desired add port of the photonic switch. $\mathbf{M_{add}}$ booster SOAs used at each input ports compensate for **PS** losses.

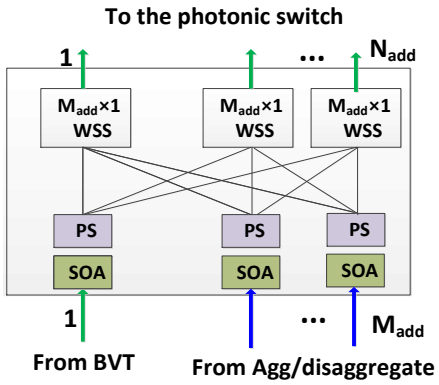

Figure 12. Architecture for the Add switch

The **PS** incurs loss that scales logarithmically with the number of output ports $\mathbf{N_{add}}$. Therefore, it could be necessary to use more than one SOA per input to compensate the PS loss for large number of output ports.

The implementation complexity of the Add switch is related the number of cross-overs which increases with the number of input ports $\mathbf{M_{add}}$ and output ports $\mathbf{N_{add}}$. On a similar note, the implementation complexity of $\mathbf{M_{add}}$ ×1 **WSS** increases with the number of the total number of unique wavelengths $\boldsymbol{\lambda_{tot}}$ and the total number of input ports $\mathbf{M_{add}}$. In the next section, the implementation details of an $\mathbf{M_{add}}$ ×1 WSS is discussed.

M_{add} × 1 WSS:

Figure 13. shows the schematic representation the architecture of $\mathbf{M_{add}}$ **× 1** WSS with two alternative configurations (option-1 and option-2). The power combiner loss in case of option-1 is 3 dB, while in option-2 it is $10log\boldsymbol{M_{add}}$.

Number of required Mux/Demux AWGs: In the first configuration, the number of deMux/Mux AWG is $\mathbf{M_{add}+1}$ while in the second configuration, the number of deMux/Mux AWGs is $\mathbf{2\times M_{add}}$.

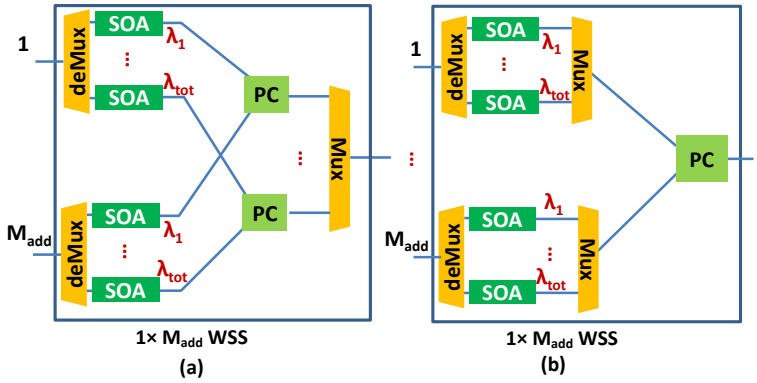

Figure 13. Architecture for the M_{add}×1 add switch (a) option-1 (b) option-2

Number of required SOAs: The number of SOAs is the same for both configurations.

Number of waveguide crossings: The number of waveguide cross-overs increases with the total number of wavelengths in option-1 while no crossing is incurred in option-2.

Estimated foot print: In option-2, increased foot print is incurred due to $\mathbf{M_{add}+1}$ number of AWGs are required.

Crosstalk: The cross-talk level in the Add switch increases with the total number of wavelengths λ_{tot}. The inter-channel cross-talk of the AWGs used in the WSS contributes to the total cross-talk level. One of the approaches of handling the accumulated crosstalk from the total number of wavelengths using a modular approach so that the cross-talk level at each output port of the module is below -35 dB.

Case study evaluation: Comparing the two configurations of an $\mathbf{M_{add}\times 1}$ WSS of the Add switch for the case study scenario definition in which 40 wavelengths spanning C-band for total capacity of 2 Tb/s per port are considered. The number of input ports M_{add}=10 (2 originate from the BVTs and 8 originate from Aggregate/disaggregate switch) and output ports is N_{add}=8. The number of required Mux/Demux AWGs is 30 and 40 for option-1 and option-2 respectively. The required number of SOAs per M_{add}×1 WSS is 400 in both cases. Due to the large number of waveguide cross-overs in Option-1, Option-2 is considered the primary option.

The target specification for the Add switch is given in Table 4. The insertion loss will be zero since a hybrid integration of the InP Add switch with SiPh interposer compensates fiber-to-chip coupling losses and the SOAs compensate on-chip losses. By ensuring PDL < 0.5 dB polarization independence is achieved.

	Unit	Target
Operational band	-	C
Insertion loss	dB	0
Loss uniformity	dB	< 1
PDL	dB	< 0.5
Cross-talk level	dB	< -35
Switching time	ms	<1
Port number	-	10x8

Table 4. Target specification of the Add switch

3.4 MULTI-CAST SWITCH: PARAMETERS AND ARCHITECTURE

The architecture of the $\mathbf{M_{MCS}\times N_{MCS}}$ *broadcast and select* MCS switch is shown in Figure. 14. It consists of $\mathbf{M_{MCS}}$ $\mathbf{1\times N_{MCS}}$ power splitters (PS) for *broadcast* operation whose losses are compensated by $\mathbf{M_{MCS}}$ booster **SOAs**. It provides a contentionless operation for a total of $\boldsymbol{\lambda_{tot}}$ wavelengths. The select operation is carried out via $\mathbf{N_{MCS}}$ $\mathbf{M_{MCS}\times 1}$ space switches. The number of cross-overs increases with the number of input ports: $\mathbf{M_{MCS}}$ and output ports: $\mathbf{N_{MCS}}$.

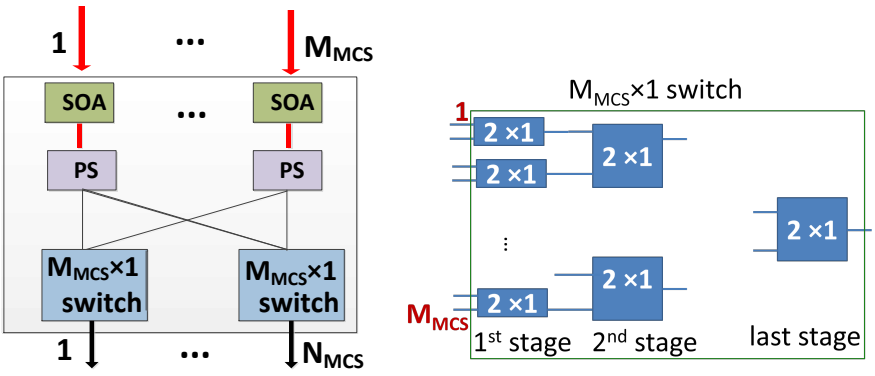

Figure 14. Architecture for the $M_{MCS}\times N_{MCS}$ MCS switch, and $M_{MCS}\times 1$ space switch

The number of input/output ports of the MCS is limited by the losses in the **PS** which scales with the number of output ports 10*log$\mathbf{N_{MCS}}$ which is compensated by the booster SOAs used per port. The maximum number of wavelengths dropped to the CRM is equal to the number of output ports $\mathbf{N_{MCS}}$. When more wavelength to be dropped more MCS modules are added.

Number of required power splitters and space switches: the number of required **PS** is equal to the number of input ports. The number of space switches scales with the number of output ports $\mathbf{N_{MCS}}$. If the space switches are implemented using MZI-SOA 2×1 switch, a single electrode per 2×1 switch is required. The number of On/Off SOAs required is twice the number of 2×1 switches.

Number of booster SOAs: the number of booster SOAs is equal to the number of input ports $\mathbf{M_{MCS}}$.

Number of waveguide crossings: The number of waveguide cross-overs increases with number of input/output ports.

Crosstalk: The cross-talk in the MCS switch is dependent on extinction ratio of $M_{MCS}\times 1$ space switches. By using either an MZI-SOA gate or SOA-gate as a switching element and limiting the number of input ports, the cross-talk can be kept below the target value of -40 dB.

Case study evaluation: For the case study scenario definition in which the $\mathbf{M_{MCS=}}8$ and $\mathbf{N_{MCS=}}16$. The number of required 8×1 space switches is 16. The required number of SOAs is 8 since the PS loss can be compensated via a single SOA per input port.

	Unit	Target
Operational band	-	C
Insertion loss	dB	0
Loss uniformity	dB	<0.5
PDL	dB	< 0.5
Cross-talk level	dB	< -40
Switching time	ms	<1
Number of 8×1 space switch		16
Port number	-	8x16

Table 5. Target specification of InP-based MCS

The target specification for the MCS is given in Table. 5. The insertion loss will be zero by since a hybrid integration of the InP MCS with SiPh interposer compensates fiber-to-chip coupling losses and the SOAs compensate on-chip losses. By ensuring PDL < 0.5 dB polarization independence is achieved. Cross-talk level below -40 dB can be realized by using in the 2×1 switch selection space switches.

3.5 COHERENT RECEIVER MODULES

In this section we focus on the realization of the CRM. The fundamental stepping stone is the submodule development, that is, realizing the monolithic integration of a dual polarization coherent receiver. This at the same time involves the development of the following building blocks (BB):

1. Narrow linewidth, widely tunable, etalon free laser to serve as local oscillator (LO)
2. On chip polarization handling structures: polarization rotator, polarization splitter/combiner
3. 90 degree hybrid with fabrication tolerances in line with the target modulation formats
4. Photodetection featuring the required >25GHz bandwidth

In the following, we address briefly some background and challenges in their realization.

Narrow linewidth, widely tunable laser: Typically, a widely integrated tunable laser consists of tunable (sampled-) Distributed feedback reflector (DBR) gratings and phase sections that can be tuned by current injection. The challenge is that with this approach, electrical noise from the current sources is translated into phase noise and therefore leads to linewidth broadening. To avoid this, we will investigate the use of thermal phase shifters, which due to the larger time constants of the thermal effects have a noise-filtering effect. Also, using InAlGaAs active layers instead of InGaAsP, has a positive effect on linewidth. Moreover, we will look at laser structures that incorporate longer cavity lengths and integrate on chip a wavelength locking mechanism. This etalon free approach will greatly simplify the packaging and favor the cost reduction.

***Polarization handling on chip*:** Much work has been done on developing integrated polarization rotators and splitters/combiners. Several concepts have been reported, either based on asymmetric waveguides or on taper-based mode converters. Most of these concepts require extra process steps and/or very accurate lithography processes. First, we will study the different concepts and assess them in terms of compatibility with the current fabrication process and robustness against process tolerances. Then we will fabricate some stand-alone devices and characterize different design variations to finally integrate the best concept.

90-degree hybrid: This component is usually realized by either a single 4x4 multi-mode interference (MMI coupler) or a sequence of cascaded 2x2 MMIs. For this component one of the main challenges is to achieve a common mode rejection ratio compliant with the modulation formats employed. Minimizing losses by design is also important. The tolerance on lithography variations will be studied with simulations. Special focus will be put on studying reflections as these can de-stabilize the local oscillator laser and there is no optical isolator between the 90-degree hybrid and the LO.

Photodetection: The current waveguide-photodetector component is based on the same layer stack as the laser and amplifier building blocks. These photodetectors already have >20GHz bandwidth. The photodetector bandwidth will be further improved by optimizing the waveguide design and the wire-bond pad layout. Implementation of balanced photodetection will be also under consideration to favor the receiver figures of merit. This can be implemented on the PIC, but there may be implementations on the isolation between the different PDs. Other options are to do the balanced detection in the electrical domain. A detailed study on the trade-offs between the two approached will be done first.
Overall, the common, and most critical challenge for the monolithic integration of the components above is that they should all be process compatible. New components either have to be compatible with the current

process flow or require very few additional process steps. The impact of fabrication tolerances will be considered as well.

The realization of the coherent receiver will be divided into two phases:

Phase I (Year 1): feasibility studies, process development and first generation of coherent receivers, which will be as a first approach, a single polarization coherent receiver.

Phase II (Year 2): integration of building blocks to assess process compatibility. When successful, the first full circuit designs will be fabricated, i.e. aiming at incorporating high spec LO and polarization handling on chip. The CRM implementation with multiple submodules will be also considered here.

3.5.1 Phase I of CRM development

In this phase, feasibility studies and process development for each building block are carried out. EFP foresees special focus on the laser and polarization handling structures.

The feasibility studies will involve simulation work and preliminary fabrication experiments. The feasibility study on laser will focus on optimizing the AlInGaAs layer stack and the integration process development as well as studying different laser architectures. The feasibility study on polarization handling will focus on developing good simulation models and assessing the fabrication tolerances.

While the process is being developed for the several building blocks, a first generation of coherent receivers will be produced, which will be as a first approach, a single polarization coherent receiver. The architecture is shown in Figure. 15. The input signal polarization control is implemented off chip and the PIC architecture offers the option to use either an external local oscillator or one internally available.

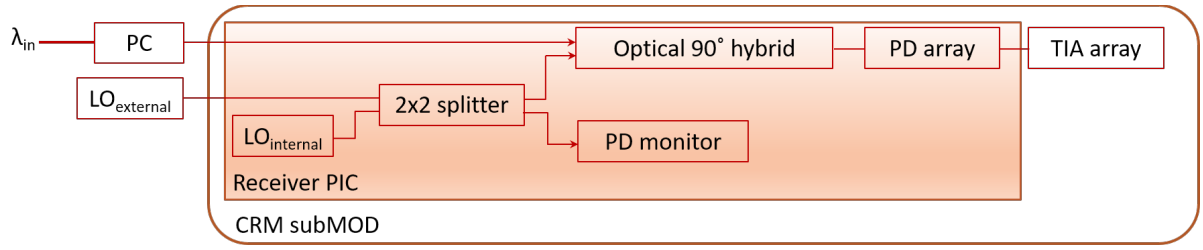

Figure 15. First generation coherent receivers' architecture, offering the option to use an external local oscillator. PC: polarization control, LO: local oscillator, PD: photodetector, TIA: transimpedance amplifier.

At the end, the expected outcomes of this phase are expected to be:

- Identify process compatibility across different building blocks ready for integration
- Optimize building block designs to achieve the required tolerances
- Implementation of first generation coherent receivers: a single polarization CO-Rx with LO having two possibilities, decoupled from CO-Rx, or integrated within CO-Rx
- Component selection for the necessary electronics (e.g. Trans impedance amplifier (TIA) array)
- Gather feedback on how to approach the multi-channel coherent receiver module

As can be seen, the target at this point goes well beyond reaching the receiver specifications. This phase is on how to reach them: process steps, design parameters, yield indication, etc. The outcomes from this phase are planned to be tested by Effect Photonics to input into the second phase of the development.

3.5.2 Phase II of CRM development

In this phase the improved BB will be co-integrated for the first time. The final design tweaks are expected to be identified and once the process compatibility and parameter choice is fixed, full coherent receiver circuits will be produced.

With these, a receiver optical subassembly (ROSA) will be designed and implemented together with the corresponding means to interface it. A breakout board will be manufactured for the latter purpose. Figure 16. shows a tentative implementation of the solution to be delivered to the project partners to conduct transmission experiments. Note that the approach for the CRM integration is yet to be determined based on preliminary subsystem performance and analysis of the packaging challenges, network requirements (modularity, scalability) and the best trade-off in cost, power, and footprint.

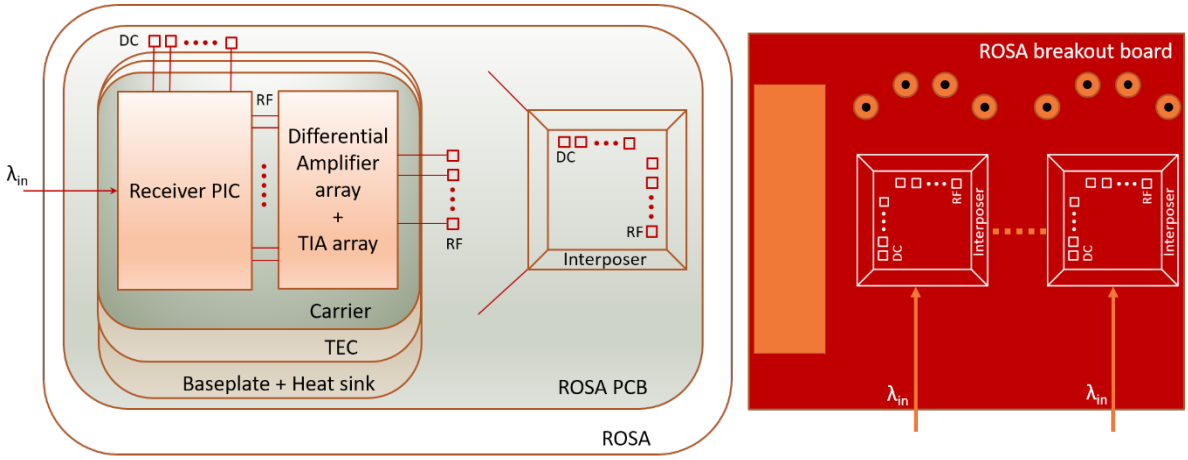

Figure 16. Sketch of the envisioned implementation of the ROSA solution (left) to be delivered to the project partners to conduct transmission experiments, employing a breakout board (right) for interfacing purposes.

Traditionally, transceivers are packaged into optical modules that are plugged into the faceplates of the networking equipment. The width of their electrical connector determines how many of these units can be plugged into a faceplate. An alternative to this approach are the board-mounted modules, the so-called on-board optics. This approach attempts to bring the optics inside, directly onto the linecards, to leverage the space and this way, achieve a higher density solution with increased thermal design flexibility. However, the maintenance and fiber management (i.e. the fiber connector of the board-mounted module to the faceplate) need to be accounted for. The Consortium for On-Board Optics (COBO) is an industry forum observing at all the relevant challenges to enable standardization of this new type of modules. Figure 17. depicts the two classes of modules discussed, pluggable and board-mounted modules.

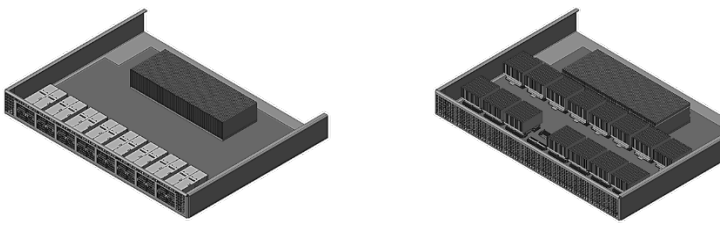

Figure 17. Two classes of optical modules: (left) pluggable optical modules, (right) board-mounted modules.

Both optical module implementations will be considered in the project to determine the most suitable approach for the CRM. While the full, compliant module implementation is out of the scope of the project, we expect to provide design-in guidelines for both options.

To summarize, the expected outcomes of this CRM development phase are:

- Integration of building blocks into a single process using the optimized design parameters found in Phase I
- Process implementation of an InAlGaAs based active layer for improved performance
- Implementation of the first full coherent receiver circuits
- Design and implementation of the ROSA solution
- Decide on the CRM approach considering the various critical figures of merit: cost, power, footprint, network needs and packaging challenges
- Deliver solution for system level testing and provide a breakout board for interfacing purposes

4 SCALABLITY, MODULARITY AND TECHNOLOGY MATCHING WITH FUNCTIONALITY

4.1 MODULARITY AND SCALABLITY

The optical switching node functionality can be upgraded by scaling with the number of input/output ports, the number of wavelengths in a single fiber (spectral multiplexing), and the number of cores in a single fiber (spatial multiplexing).

Scaling to high wavelength count: due to high capacity requirement the total number of unique wavelengths channels λ_{tot} (can be more than 100 wavelengths). This poses a limitation in the available gain per wavelength in booster amplifiers, and the size and complexity of a single WSS to be realized in a single PIC. To solve this, an interleaver is used to slice the number of wavelength channels and a separate switching module is used to process each of interleaver outputs. The number of spectral slices generated by the interleaver has an even count for ease of implementation (M_o=2,4,6,...) .

Figure 18. (a) and (b) show the typical modular approach of scaling the Aggregate/disaggregate switch and the Add switch for large wavelength count cases. An interleaver per input port of the Aggregate/disaggregate switch generates M_o spectral bands. The total number of wavelengths handled by a single 1×2 WSS is reduced λ_{tot}/M_o. As a result, the total number of outputs of the Aggregate/disaggregate switch is increased from N_{agg} to $M_o \times N_{agg}$ because of the spectral slicing. The output ports connected to the Add switch are $1/2 \times M_o \times N_{agg}$. Because of the increased number of input ports by M_o times at the Add switch, M_o separate Add switch modules are used as shown in Fig. 18(b). At the output, M_o multiplexing units are used, resulting N_{add} switch ports which are connected to the add ports of the photonic switch.

Scaling to high port count: the high port count of the switches demanded by the high capacity requirement poses a limitation on the number of ports that are practically realizable in a single PIC per switching functionality. The main limitation comes from power splitter losses, the number of SOAs required, as well increased form factor and the size and complexity of the WSS elements. To combat this implementation obstacle an array of switching modules is used. On the other hand, reduced switching flexibility is incurred (i.e. not being able to reach any output port from any input port). This can be solved by using a separate shuffling network for interconnectivity between the modules at a cost of slight increase in complexity.

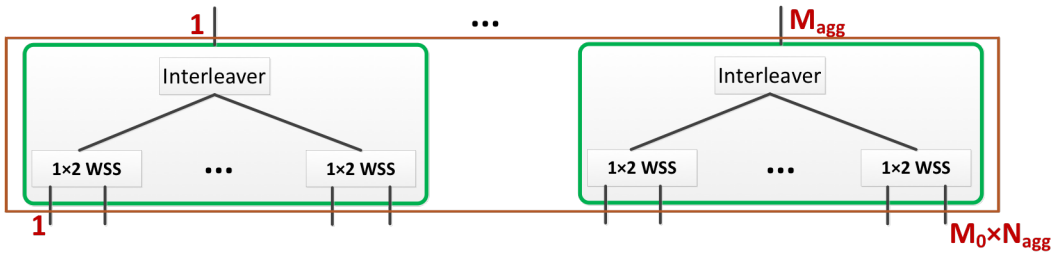

(a)

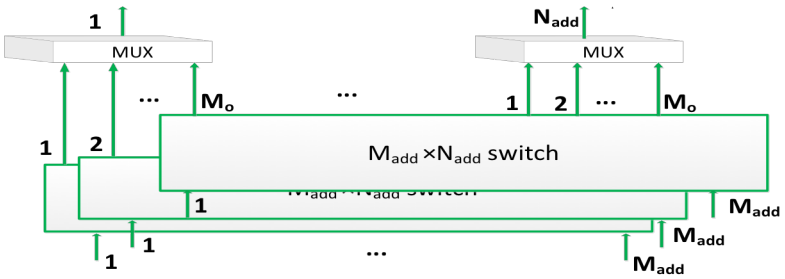

(b)

Figure 18. (a) Modular design of the Aggregate/disaggregate switch for high wavelength count cases. (b) Modular design of the Add switch where spectral slices are handled by different switching modules

A typical case of scaling to high port count implementation involves modular design of MCS so as to increase the total number of output ports. For a total number of wavelengths λ_{tot} input at **MCS,** a single MCS module can drop only N_{MCS} number of wavelengths at a time. N_{MCS} is only limited to 24 in practice[22] thereby limiting the number of dropped wavelengths. Figure 19. shows the modular design of an MCS when the number output ports is increased so as to increase the number of wavelengths to be dropped.

The number of output ports of an MCS is limited by the loss in the **PS** and required number SOA elements for compensating the loss. In order to increase the number of wavelengths, array of M_0 MCS modules are used together as shown in Figure 19. First the output of each input port is amplified by an SOA and split by **1× M_0** PS. A shuffle network distributes a copy of the input signal to each of MCS modules where a **M_{MCS}×1** switch is used to select one signal. In this way the maximum number of dropped wavelengths is increased to **N_{MCS}× M_0.**

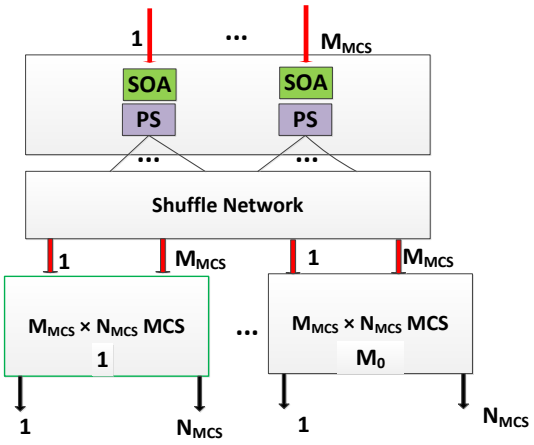

Figure 19. Modular design of MCS, to expand the number of output ports to $M_o \times N_{MCS}$

Space Division Multiplexing (SDM) approach: Space division multiplexing (SDM) over multi-core fibers (MCF) would allow the network capacity to scale to orders of magnitude higher than what can be achieved with an SMF-based network infrastructure.

In the PASSION project, we adopt an approach where the use of MCF high capacity connectivity between nodes. That means the express traffic by MCF each carrying N_c number of cores. So far the number of cores that can be realized is 31 and recently ultra dense implementation with 64 cores is reported[23].

A super architecture of the PASSION optical switching node when MCF input and output fibers are employed is shown in Figure 20. The input/output ports of the photonic switch are equipped with MCF each of which carries N_c cores. The MCF are fanned in and out at the in the input and outputs of the photonic switch. The connection between Photonic switch and Add, MCS and Aggregate/disaggergate switch is handled by SMF. The number of input fibers to Aggregate/disaggreggate switch is $N_c \times M_{agg}$. Because of the increased number of WDM channels with space division multiplexing, N_c separate modules of the Aggregate/disaggregate switch are used to handle the overall traffic and to scale performance.

As described before, scalability to a high wavelength count is adopted via the use of interleavers per input port of the Aggregate/disaggregate switch. To support the spectral and spatial scalability the number of input SMF increases to $N_c \times M_{agg}$ and the number of output SMF to $N_c \times M_o \times N_{agg}$. $M_o \times N_c \times M_{agg}$ output fibers of the Aggregate/disaggregate switch colored in blue are connected to the Add switch and the remaining $N_c \times M_o \times M_{agg}$ output fibers colored in red are connected to the MCS.

On a similar note, by adopting modularity approach, all the switching functionalities at the Add switch and MCS are duplicated via the use of $N_c \times M_o$ arrays of modules. The number of modules of the Add switch is $N_c \times M_o$ *and* $M_{add} \times N_c$ spectral multiplexers are used to spectrally aggregate the Add switch modules.

The modularity in the MCS is scaled by having N_c MCS modules each of which contains M_c MCS sub-modules whose input are connected via shuffle networks, in which all M_{MCS} input ports can be dropped to $M_c \times N_{MCS}$ output ports, thereby allowing to drop $M_c \times N_{MCS}$ wavelengths. The N_c modules allow dropping a total of $N_c \times M_c \times N_{MCS}$ wavelengths.

Number of switching components per node: The number of required switching sub-components per node depends on the level of spectral and spatial granularity adopted (the total number of wavelength channels λ_{tot} and the number of cores per fiber N_c which determines the node capacity and the number of input/output ports at each switching stage). Table 6(a) and Table 6(b) summarize the required number of switching subcomponents for optical switching nodes with a capacity of 2 Tb/s and 56 Tb/s per link respectively and 32 Tb/s and 896 Tb/s per node respectively.

Parameters	Symbol representation	Sub -components	amount
Node capacity			2 Tb/s
Total number of cores per fiber	N_c		1
Total number of unique wavelengths	λ_{tot} (M_0=1)		40
Number of interleavers and deMux			0
Number of ports of the Photonic switch	[M_{ph} , N_{ph}]= [16,16]	TIR electrodes	256
		Photonic switch module	1
Number of ports of the aggregate switch	[M_{agg} , N_{agg}]=[8,16]	1×2 WSS	8
		Agg/disaggregate switch module	1
Number of ports at the Add switch	[M_{add},N_{add}]=[10,8]	10×1 WSS	8
		Booster SOAs	10
		1×8 PS	10
		Add switch module	1
Number of ports at the MCS	[$M_{Mcs,}$$N_{MCS}$]=[8,16]	1×16 PS	8
		Booster SOAs	8
		8×1 switch	16
		MCS switch module	1
Total number of receivers /end users			16

Table 6 (a) Number of required switching components for 2 Tb/s per link and 32 Tb/s per switching node

Parameters	Symbol representation	Sub -components	amount
Node capacity			56 Tb/s
Total number of cores per fiber	N_c		7
Total number of wavelengths	λ_{tot}		160
Total number of spectral slices	M_0		4
Number of interleavers & deMux			7×8
Number of ports of the Photonic switch	[M_{ph} , N_{ph}]= [16,16]	TIR electrodes	256
		Photonic switch module	1
Number of ports of the aggregate switch	[M_{agg} , N_{agg}]=[8,16]	1×2 WSS	8×4×7
		Agg/disaggregate switch module	7
Number of ports at the Add switch	[M_{add},N_{add}]=[10,8]	10×1 WSS	8×4×7
		Booster SOAs	10×4×7
		1×8 PS	10×4×7
		Add switch module	4×7
Number of ports at the MCS	[$M_{Mcs,}$$N_{MCS}$]=[8,16]	1×16 PS	8
		Booster SOAs	40 ×7
		8×1 switch	16
		MCS module	7
		Mc	1
Total number of receivers /end users			16×4×7

Table 6 (b) Number of required switching components for 56 Tb/s per link and 896 Tb/s per node

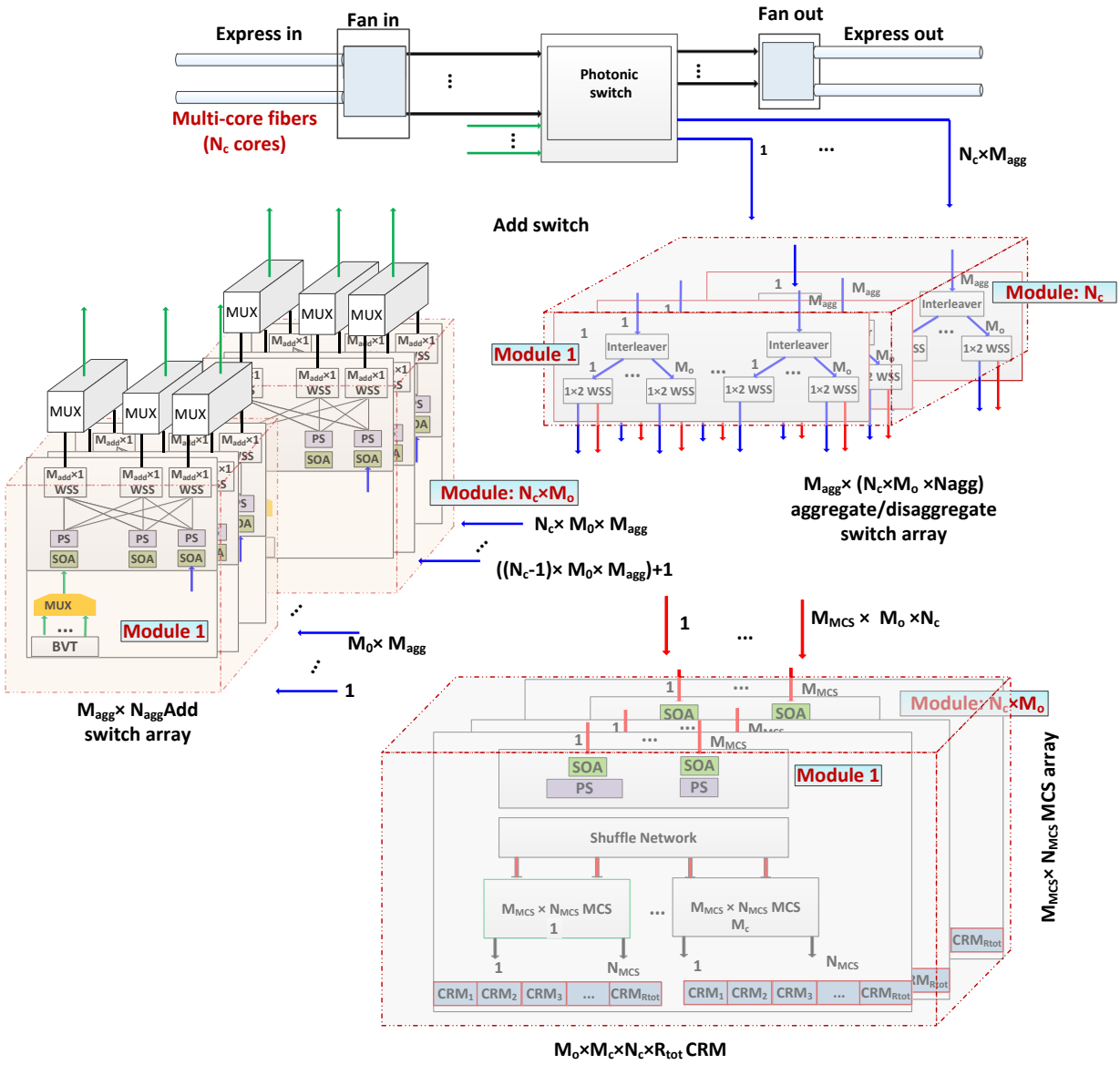

Figure 20. Modular architecture of the PASSION switching node in consideration of spectral and spatial scalability, subcomponent functionalities are scaled in modularity basis

4.2 SCALABLITY EVALUATION

In this section, the scalablity of the switching node architecture presented in the last section is evaluated with regard to the power consumption and the total optical cross-talk.

Power consumption vs the number of input ports: The power consumption of the Aggregate/ disaggregate switch which involves the use of M_{agg} 1× 2 WSS. The power consumption calculation takes into consideration that the InP SOA gate switches consume 200 mW, half-length shorter SOA gate switches consume 100 mW for a given length and bias current conditions. The overall power consumption of the Aggregate/disaggregate switch vs the number of input ports M_{agg} is given in Figure 21. (a) and (b) for 40 and 160 wavelengths respectively.

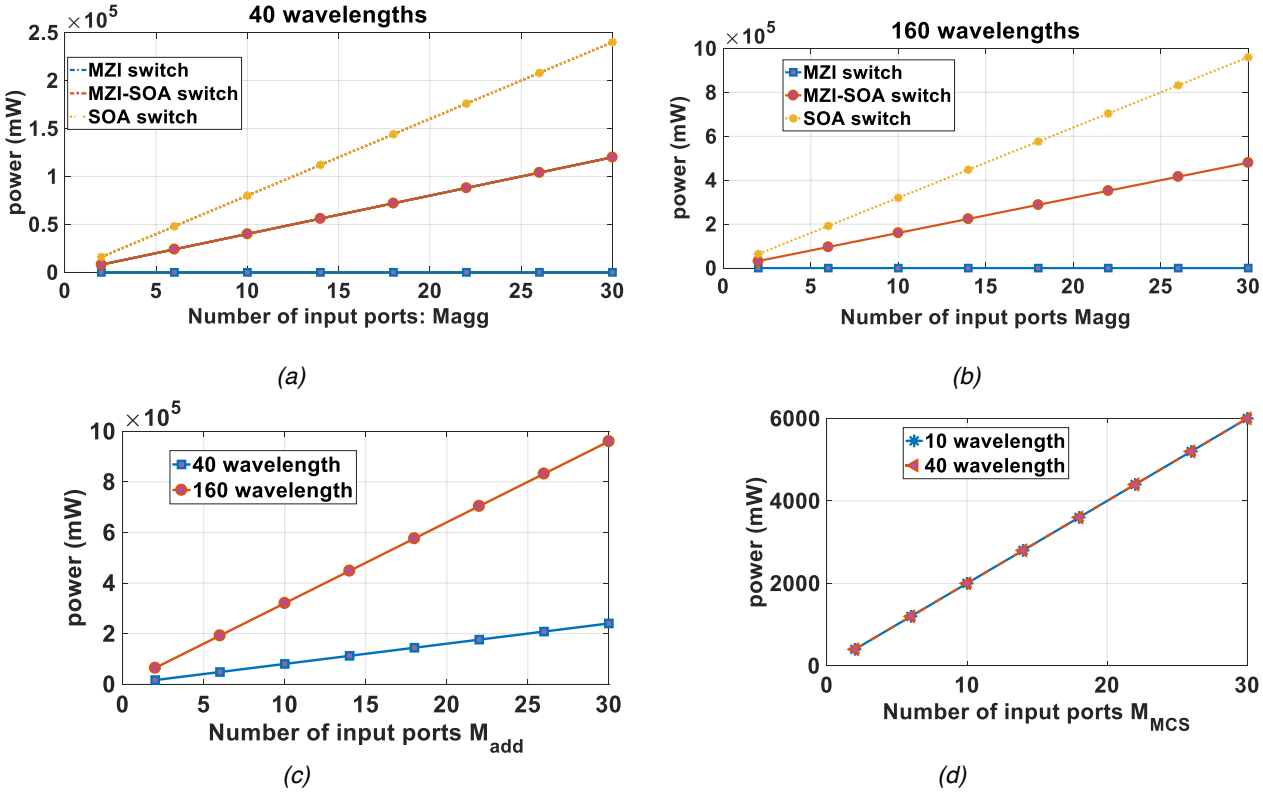

Figure 21. Electrical power consumption as a function of the number of input ports (a) aggregate/disaggregate switch for 40 wavelengths (b) 160 wavelengths (c) M_{add} ×1 WSS in the Add switch (d) power consumption of the booster SOA in MCS

Comparing the difference in using either SOA gate switch vs MZI-SOA switch brings 1.2×10^2 W difference in the power consumption when the number of input ports $\mathbf{M_{agg}}$=30. This difference increases to 4.8×10^2 W when the number of wavelength increases to 160. Using only MZI based switches does not have any power consumption but suffers from a large cross-talk level in the order of -20 dB. Figure 21. (c) shows the power consumption in mW in the M_{add} ×1 switches as a function of number of input ports M_{add}. Due to the increase in the number of used SOA gates the power consumption linearly scales with the wavelength count. In Figure 21. (d), the power consumption due to booster SOA as a function of input port number: M_{MCS} is plotted. The power consumption of the booster SOAs is independent of the number of wavelengths.

Cross-talk vs the number of input ports: the cross-talk level at the single output port of a switch originates from the poor isolation across all the switching paths. The cross-talk accumulation increases as a function of paths being combined at a multiplexer and power combiner. The Add switch functionality is analyzed by considering the end-to-end cross-talk level of a single wavelength path in **M_{add}×1** WSS architecture presented in Figure 13. (b). Considering a -60-dB cross-talk level of a single wavelength path, the overall cross-talk after the power combiner at each output port is calculated.

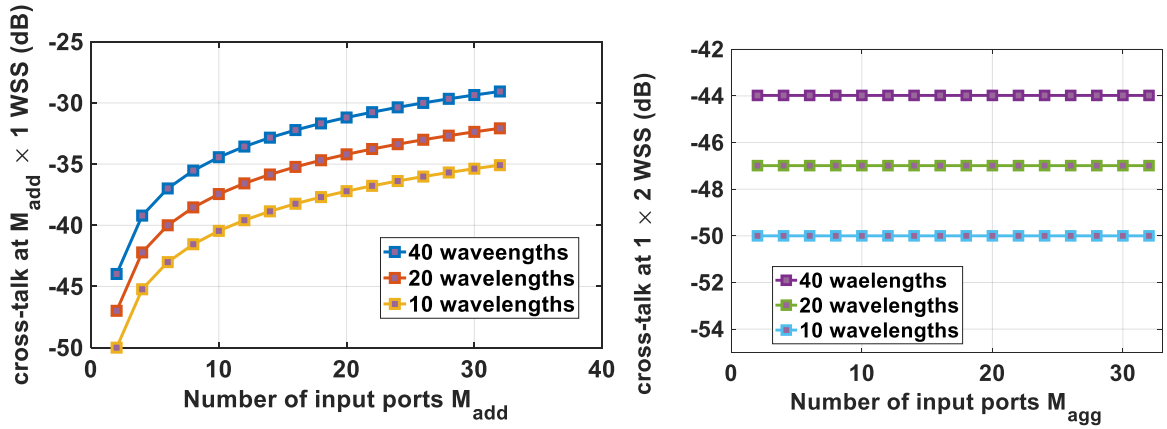

Figure 22. Total optical cross-talk (a) At the output of Add switch (b) At the output port of Agg/disaggregate switch

Figure 22. (a) shows the cross-talk level at each output port of the Add switch per increasing input port **M_{add}** count when the considered total number of wavelengths is λ_{tot}=10, 20, and 40. On the other hand, the cross-talk level on the Aggregate/disaggregate switch does not increase with the number of input ports M_{agg}. Comparing the cross-talk for cases of 40, 20, 10 wavelengths, the cross-talk is higher for 40 wavelengths as expected.
Evaluating the calculated values for the power consumption and cross-talk level, it is recommended to keep to the number of input ports M_{add} and M_{agg} below 10 and number of wavelengths below 40 in a single Add switching module and Aggregate/disaggregate switching modules so that the cross-talk level is below -40 dB.

4.3 TECHNOLOGY MATCHING WITH FUNCTIONALITY OF THE SUBCOMPONENTS

In this section, the main functionalities employed in the switching components together with the target technology implementation platform are enlisted in Table 7.

The multiplexing/demultiplexing elements implemented as AWGs together with the On/Off SOA gate switches are implemented in InP platform due to the high technology readiness available in the clean room environment in Technical University of Eindhoven. Smaller scale WSS based on AWG Mux/demux, SOA gates, splitting and shuffling functionalities are already demonstrated in InP platform as documented in the publication[24,25]. As a result, the Add switch, MCS, Aggregate/disaggregate switches will be implemented in InP platform due to ability to integrate all the active and passive elements of the sub-systems.

On-chip SOAs compensate for the losses within the chip, while hybrid integration of InP with Siph interposer will be used for lossless coupling with SMF. For high port count photonic space switches implementation polymer PLC from ETRI has been selected due to the low cost fabrication and small footprint.

Switch	Multiplexing/ demultiplexing	SOA Gating	Splitting and Shuffling	(N×M) space switching	Technology
Add switch	×	×	×		InP
Multi-cast switch			×	×	InP
Photonic Space switch				×	Polymer PLC
Aggregate/disaggregate switch	×	×	×		InP

Table 7. Technology matching with functionality of the subcomponents

5 CONCLUSIONS

This deliverable reports the architecture of the high capacity optical switching node and the related sub-systems to provide flexible add/drop, and aggregation functionalities. These devices increase the network and system scalability, programmability and re-configurability. A photonic switching matrix provides 'high level switching' between the express and add/drop traffic without considering the spectral granularity dimension. The Aggregate/disaggregate switch functionality supports the flexible resource utilization by aggregating/ disaggregating traffic to be re-routed back to the express traffic or to the drop path. An array of multi-cast switches enable efficient utilization of the coherent receiver modules.

The modularity principle employed in the optical node implementation allows for scalable performance in pay-as-you-grow principle. In this way, each switching module has an acceptable physical size and physical impairments (such as splitter losses and cross-talk) depending by the exploited signal modulation format. The level of granularity and the system architecture are determining factors in the number of required switching modules and the number of sub-components in each switching module.

6 REFERENCES

[1] Photonic21 reports, www.photonics21.org

[2] Ovum, "Optical Networks Forecast Report: 2016-2021"

[3] Dell'Oro, "Optical Transport Quarterly Report 4Q2016"

[4] M. Lauermann, et al., "Multi-Channel , Widely-Tunable Coherent Transmitter and Receiver PICs Operating at 16-QAM," in *OFC/NFOEC 2017 - PDP – Los Angeles CA 2017*

[5] A. Himeno, R. Nagase, T. Ito, K. Kato, and M. Okuno, "Photonic inter-module connector using 8x8 optical switches for near-future electronic switching systems," IEICE Trans. Commun. E77-B(2), 155-162 (1994).

[6] M. C. Wu, O. Solgaard, and J. E. Ford, "Optical MEMS for lightwave communication," IEEE J. Lightw. Technol. 24(12), 4433-4454 (2006).

[7] J. E. Fouquet, "Compact optical cross-connect switch based on total internal reflection in a fluid-containing planar lightwave circuit," in Proceedings Opt. Fiber Commun. Conf. Tech. Dig. Post conference Edition. Trends Opt. and Photon. 37, (Washington, DC, 2000), pp. 204-206.

[8] T. Goh, A. Himeno, M. Okuno, H. Takahashi, and K. Hattori, "High-extinction ration and low-loss silica-based 8x8 thermo-optic matrix switch," IEEE Photon. Technol. Lett. 10(3), 358-360 (1998).

[9] T. Goh, A. M. Yasu, K. Hattori, A. Himeno, M. Okuno, Y. Ohmori, "Low loss and high extinction ratio strictly non-blocking 16x16 thermo-optic matrix switch on 6-in wafer using silica-based planar lightwave circuit technology," IEEE J. Lightw. Technol. 19(3), 371-379 (2001).

[10] Y.-T. Han, J.-U. Shin, S.-H. Park, S.-P. Han, C.-H. Lee, Y.-O. Noh, H.-J. Lee, and Y. Baek, "Crosstalk- enhanced DOS integrated with modified radiation-type attenuators," ETRI Journal, 30(5), 744-746 (2008).

[11] Y.-T. Han, J.-U. Shin, S.-H. Park, S.-P. Han, Y. Baek, C.-H. Lee, Y.-O. Noh, H.-J. Lee, and H.-H. Park, "Fabrication of 10-channel polymer thermo-optic digital optical switch," IEEE Photon. Technol. Lett. 21(20), 1556-1558 (2009).

[12] J.-U. Shin, Y.-T. Han, S.-P. Han, S.-H. Park, Y. Baek, Y.-O. Noh, and K.-H. Park, "Reconfigurable optical add-drop multiplexer using a polymer integrated photonic lightwave circuit," ETRI Journal, 31(6), 770-777 (2009).

[13] R. Hauffee, U. Siebel, and K. Petermann, "Crosstalk-optimized integrated optical switching matrices in polymers by use of redundant switch," IEEE Photon. Technol. Lett. 13(3), 200-202 (2001).

[14] X. Wang, B. Howley, M. Y. Chen, and R. T. Chen, "4x4 non-blocking polymeric thermo-optic switch matrix using the total internal reflection effect," IEEE J. Select. Topics. Quantum Electron. 12(5), 997-1000 (2006).

[15] Y.-T. Han, J.-U. Shin, S.-H. Park, S.-P. Han, Y. Baek, C.-H. Lee, Y.-O. Noh, and H.-H. Park, "Polymer 1x2 thermo-optic digital optical switch based on the total-internal-reflection effect," ETRI Journal, 33(2), 275-278 (2011).

[16] R. V. Penty, M. Ding, A. Wonfor, and I. H. White, "Scaling of Low Energy InP SOA Based Switches," in Advanced Photonics 2017 (IPR, NOMA, Sensors, Networks, SPPCom, PS), OSA Technical Digest (online) (Optical Society of America, 2017), paper PM4D.3.

[17] Q. Cheng, A. Wonfor, R. V. Penty and I. H. White, "Scalable, Low-Energy Hybrid Photonic Space Switch," in Journal of Lightwave Technology, vol. 31, no. 18, pp. 3077-3084, Sept.15, 2013.

[18] B. Lee and A. Rylyakov, "Four-and eight-port photonic switches monolithically integrated with digital CMOS logic and driver circuits," presented at the Opt. Fiber Commun. Conf. Expo. Nat. Fiber Opt. Eng. Conf., Anaheim, CA, USA, 2013, Paper PDP5C.3.

[19] J. Van Campenhout, W. M. J. Green, S. Assefa, and Y. A. Vlasov, "Lowpower, 2×2 silicon electro-optic switch with 110-nm bandwidth for 3084 JOURNAL OF LIGHTWAVE TECHNOLOGY, VOL. 31, NO. 18, SEPTEMBER 15, 2013 broadband reconfigurable optical networks," Opt. Exp., vol. 17, no. 26, pp. 24020–24029, 2009.

[20] H. Bukkems and C. Herben, "Minimization of the loss of intersecting waveguides in InP-based photonic integrated circuits," IEEE Photon.Technol. Lett., vol. 11, no. 11, pp. 1420–1422, Nov. 1999.

[21] C. Van Dam and F. Van Ham, "Low-crosstalk and low-loss waveguide crossings on InP with small dimensions," Fiber Integr. Opt., vol. 16, pp. 83–87, 1997.

[22] W. I. Way, "Optimum architecture for M×N multicast switch-based colorless, directionless, contentionless, and flexible-grid ROADM," OFC/NFOEC, Los Angeles, CA, 2012, pp. 1-3.

[23] B. Li, M. Tang, L. Huo, L. Deng, S. Fu, and P. P. Shum, "64 Core Ultra Dense Multicore Fiber Design for Optical Fronthaul Systems," in Advanced Photonics 2016 (IPR, NOMA, Sensors, Networks, SPPCom, SOF), OSA Technical Digest (online) (Optical Society of America, 2016), paper SoM2F.2.

[24] R. Stabile, A. Rohit, and K. A. Williams, "Monolithically integrated 8×8 space and wavelength selective crossconnect," J.Lightwave Technol. 32(2), 201–207 (2013)

[25] N. Calabretta, W. Miao and K.A. Williams, "Nanosecond wavelength and space optical crossconnect switches for high performance optical switches", 18th International Conference on Transparent Optical Networks (ICTON), Trento, Italy, July 10-14,2016.

7 ACRONYMS

AWG - ARRAYED WAVE GUIDE GRATING

BBU-BASE BAND UNIT

BVT - BANDWIDTH VARIABLE TRANSMITTER

CDC - COLORLESS/DIRECTIONLESS/CONTENTION LESS

CPRI- COMMON PUBLIC RADIO INTERFACE

COBO- CONSORTIUM ON BOARD OPTICS

CRM - COHERENT RECEIVER MODULE

DBR- DISTRIBUTED FEEDBACK REFLECTOR

DC- DATA CENTER

DEMUX -DEMULTIPLEXER

EON - ELASTIC OPTICAL NETWORK

ICT- INFORMATION COMMUNICATIONO TECHNOLOGY

MCF-MULTI-CORE FIBER

MCS -MULTI-CAST SWITCHES

MTC- MACHINE TYPE COMMUNICATION

MUX - MULTIPLEXER

MZI-MACH-ZEHNDER INTERFEROMETER

OLT- OPTICAL LINE TERMINAL

ONU- OPTICAL NETWORK UNIT

OSNR - OPTICAL SIGNAL TO NOISE RATIO

PIC-PHOTONIC INTEGRATED CIRCUIT

PLC -PLANAR LIGHT WAVE CIRCUIT

PON-PASSIVE OPTICAL NODE

POP-POINT OF PRESENCE

PS - POWER SPLITTER

PTP-POINT-TO-POINT

RAN- RADIO ACCESS UNIT

ROADM-RECONFIGURABE ADD/DROP MULTIPLEXER

ROSA-RECEIVER OPTICAL ASSEMBLY

SBVT-SLICEABLE BVT

SDM -SPACE DIVISION MULTIPLEXING

SDN-SOFTWARE DEFINED NETWORK

SIPh- SILICON PHOTONICS

SMF - SINGLE MODE FIBER

TE- TRANSVERSE ELECTRIC

TIA- TRANS-IMPEDANCE AMPLIFIER

TIR- TOTAL INTERNAL REFLECTION

TWDM- TIME MULTIPLEXED WDM

URLLC- ULTRA RELIABLE AND LOW-LATENCY COMMUNICATION

VCSEL - VERTICAL SERFACE EMITTING LASERS

VNFI-VIRTUALIZED NETWORK FUNCTION INFRASTRUCTURE

WDM- WAVELENGTH DIVISION MULTIPLEXING

WSS -WAVELENGTH SELECTIVE SWITCH